Biogeosciences Discuss., 11, 8861–8923, 2014
www.biogeosciences-discuss.net/11/8861/2014/
doi:10.5194/bgd-11-8861-2014

Biogeosciences Discussions
Open Access

Pasture degradation modifies the water and carbon cycles of the Tibetan highlands

W. Babel[1], T. Biermann[1,*], H. Coners[2], E. Falge[1], E. Seeber[3], J. Ingrisch[4,], P.-M. Schleuß[4], T. Gerken[1,5,***], J. Leonbacher[1], T. Leipold[1], S. Willinghöfer[2], K. Schützenmeister[6], O. Shibistova[7,8], L. Becker[7], S. Hafner[4], S. Spielvogel[4,6], X. Li[9], X. Xu[4,10], Y. Sun[4,10], L. Zhang[11], Y. Yang[12], Y. Ma[11], K. Wesche[3,13], H.-F. Graf[5], C. Leuschner[2], G. Guggenberger[7], Y. Kuzyakov[4,14,15], G. Miehe[16], and T. Foken[1,17]**

[1]University of Bayreuth, Department of Micrometeorology, Bayreuth, Germany
[2]University of Göttingen, Department of Plant Ecology and Ecosystem Research, Göttingen, Germany
[3]Senckenberg Museum Görlitz, Department of Botany, Görlitz, Germany
[4]University of Göttingen, Department of Soil Sciences of Temperate Ecosystems, Göttingen, Germany
[5]University of Cambridge, Department of Geography, Centre for Atmospheric Science, Cambridge, UK

[6]University of Koblenz-Landau, Institute of Integrated Environmental Sciences, Koblenz, Germany
[7]Leibniz Universität Hannover, Institute for Soil Science, Hannover, Germany
[8]V. N. Sukachev Institute of Forest, Krasnoyarsk, Russia
[9]School of Life Sciences, Lanzhou University, Lanzhou, China
[10]Chinese Academy of Sciences, Institute of Geographical Sciences and Natural Resources Research, Beijing, China
[11]Chinese Academy of Sciences, Institute of Tibetan Plateau Research, Key Laboratory of Tibetan Environment Changes and Land Surface, Processes, Beijing, China
[12]Chinese Academy of Sciences, Institute of Tibetan Plateau Research, Laboratory of Alpine Ecology and Biodiversity Focuses, Processes, Beijing, China
[13]German Centre for Integrative Biodiversity Research (iDiv) Halle–Jena–Leipzig, Germany
[14]University of Göttingen, Department of Agricultural Soil Science, Göttingen, Germany
[15]Institute of Environmental Sciences, Kazan Federal University, Kazan, Russia
[16]University of Marburg, Faculty of Geography, Marburg, Germany
[17]Member of Bayreuth Center of Ecology and Ecosystem Research, Bayreuth, Germany
[*]now at: Lund University, Centre for Environmental and Climate Research, Lund, Sweden
[**]now at: University of Innsbruck Institute of Ecology Research, Innsbruck, Austria
[***]now at: The Pennsylvania State University, Department of Meteorology, University Park, PA, USA

Received: 21 May 2014 – Accepted: 29 May 2014 – Published: 12 June 2014

Correspondence to: T. Foken (thomas.foken@uni-bayreuth.de)

Published by Copernicus Publications on behalf of the European Geosciences Union.

Abstract

The Tibetan Plateau has a significant role with regard to atmospheric circulation and the monsoon in particular. Changes between a closed plant cover and open bare soil are one of the striking effects of land use degradation observed with unsustainable range management or climate change, but experiments coupling changes of surface properties and processes with atmospheric feedbacks are rare and have not been undertaken in the world's two largest alpine ecosystems, the alpine steppe and the *Kobresia pygmaea* pastures of the Tibetan plateau. We coupled measurements of microlysimeter, chamber, ^{13}C labeling, and eddy-covariance and combined the observations with land surface and atmospheric models, adapted to the highland conditions. This allowed us to analyze how three degradation stages affect the water and carbon cycle of pastures on the landscape scale within the core region of the *Kobresia pygmaea* ecosystem. The study revealed that increasing degradation of the *Kobresia* turf affects carbon allocation and strongly reduces the carbon uptake, compromising the function of *Kobresia* pastures as a carbon sink. Pasture degradation leads to a shift from transpiration to evaporation while the total sum of evapotranspiration remains unaffected. The results show an earlier onset of convection and cloud generation, likely triggered by enhanced evaporation. Consequently, precipitation starts earlier and clouds decrease the incoming solar radiation. In summary, the changes in surface properties by pasture degradation found on the highland have a significant influence on larger scales.

1 Introduction

Alpine ecosystems are considered as highly vulnerable to the impact of climate and land use change. This is especially the case for two of the world's highest and largest alpine ecosystems: the *Kobresia pygmaea* pastures covering 450 000 km^2 in the southeast and the alpine steppe covering 600 000 km^2 in the northwest of the Tibetan Plateau. The *Kobresia pygmaea* pastures typically form a closed grazing lawn of about

2 cm in height with up to 98 % cover of *Kobresia pygmaea*, as main constituent of a felty turf (Kaiser et al., 2008; Miehe et al., 2008b). The alpine steppe is a central Asian short grass steppe with alpine cushions and a plant cover declining from 40 % in the east to 10 % in the west (Miehe et al., 2011). Both ecosystems are linked by an ecotone of 200 km in width over 2000 km length (Fig. 1).

Obvious features of degradation in the *Kobresia* pastures and their ecotone are controversially discussed as being caused by either natural abiotic and biotic processes or human impacts (Zhou et al., 2005). The most widespread pattern are mosaics of (i) closed *Kobresia* grazing lawns (later named as Intact root Mat, IM), (ii) root turf that is only sparsely vegetated by *Kobresia pygmaea* but sealed with Cyanophyceae (later named as partly Degraded root Mat, DM), and (iii) open loess and gravels that are sparely colonised by cushions, rosettes and small grasses of the alpine steppe (later named as Bare Soil, BS).

Assessments of pasture degradation have been either based on biotic parameters such as decreasing vegetation cover, species diversity, productivity and forage quality, or alternatively on abiotic factors including nutrient loss, soil compaction and ongoing soil erosion (Harris, 2010). A definition of degradation stages was given by Liu et al. (2003) and later on used by Zhou et al. (2005). According to a study by Niu (1999), 30 % of the *Kobresia* grassland is degraded at various levels. Holzner and Kriechbaum (2000) reported that about 30 % is in optimal condition, about 30 % shows characteristics of overgrazing where regeneration seems to be possible after improved utilisation and about 40 % shows recent or ancient complete degradation. Here, we regard bare silty soil as the final degradation stage of a former *Kobresia* pasture with its intact root turf. Loss of *Kobresia* cover goes along with a decrease of palatable species and thus pasture quality.

The general lack of data on the alpine ecology of *Kobresia* pastures is in strong contrast to the relevance of this ecosystem. However, it is important not only to gain more knowledge on single aspects of the *Kobresia* pasture, but especially on ecological functions of the ecosystem. Therefore, modelling of the effects of degradation on

atmospheric processes as well as more general analysis of interactions is necessary (Cui and Graf, 2009). Only when this challenge has been met can the effect be investigated in climate models, both for the past, but mainly for a future climate. Therefore, there is an urgent need to identify the parameters and factors influencing the pastures and to quantify energy and matter fluxes.

In order to model fluxes over *Kobresia* and degraded areas, it is necessary to identify those model parameters which change significantly due to any degradation present. Three parameters could reflect these problems:

- Missing vegetation: the difference is considered in the simulation through the fraction of vegetated areas and the respective parameter differences between bare soil evaporation and grassland evapotranspiration, as well as assimilation and respiration.
- Different soil properties: due to the missing *Kobresia* turf, soil properties of the upper layer might be changed: less living and dead organic material lead to poor isolation and switch from hydrophobic to more hydrophilic properties, thus leading to higher infiltration capacity and higher soil hydraulic conductivity.
- The available energy changes mostly due to albedo differences and outgoing longwave radiation. Furthermore, the direct solar irradiation is much larger than diffuse radiation compared to other regions of the world.

Degradation of vegetation and soil surface at the plot scale leads to changes of water and carbon fluxes, as well as carbon stocks, at the ecosystem level, with consequences for the whole Tibetan plateau. The aim of this study was to analyze and model for the first time the water and carbon fluxes in the above-mentioned three types of surface patterns of *Kobresia* pastures on the Tibetan Plateau. We combine the benefits of observing water and carbon fluxes at the plot scale, using micro-lysimeter, chamber-based gas exchange measurements and $^{13}CO_2$ labelling studies, and also simultaneously at the ecosystem scale with eddy-covariance measurements. Our model studies

are focused on land surface models, where the description of plant and soil parameters is more explicitly parameterized than in larger-scale models. They bridge between the plot and the ecosystem scale and simulate the influence of increasing degradation on water and carbon fluxes, which ultimately leads to changes of cloud cover and precipitation.

2 Material and methods

2.1 Study sites

For the present study, measurements were taken at three study sites on the Tibetan plateau. Details are given in Table 1. For the experimental activities at the sites see Sect. 2.5.

Xinghai: The experimental site is located in Qinghai province in the northeastern Tibetan Plateau, approximately 200 km southwest of Xining, and about 15 km south of Xinghai city. The montane grassland has developed on a loess-covered (1.2 m) terrace of the Huang He River. The grassland is used as a winter pasture for yaks and sheep for 6–7 months of the year (Miehe et al., 2008b; Unteregelsbacher et al., 2012). About 20 % of the pasture at the experiment site is completely covered with blue-green algae and crustose-lichens.

Kema: The "*Kobresia pygmaea* Research Station Kema", established in 2007, is located in the core area of alpine *Kobresia pygmaea* pasture. All measurements were established either within or in the close surroundings of an area of 100 m by 250 m, fenced in 2009, on a pasture where grazing was restricted to a few months during winter and spring. The growing season strongly depends on the availability of water, and usually starts at the end of May with the onset of the monsoon and ends with longer frosts by the end of August or September. *Kobresia pygmaea* has an average

vegetation grazed height of 1–2 cm (Miehe et al., 2008b) and forms a very tough felty root turf of living and dead *Kobresia* roots, leaf bases and soil organic matter (Kaiser et al., 2008). It is designated as *Kobresia* root mat throughout this study and attains a thickness of 14 cm.

The site is covered with *Kobresia pygmaea* (Cyperaceae), accompanied by other monocotyledons (*Carex ivanoviae*, *Carex* spp., *Festuca* spec., *Kobresia pusilla*, *Poa* spp., *Stipa purpurea*) and to a minor degree by perennial herbs. For more details on the species diversity see Biermann et al. (2011, 2013).

Nam Co: The "Nam Co Monitoring and Research Station for Multisphere Interactions" (NAMORS) of the Institute of Tibetan Plateau Research of the Chinese Academy of Science (Ma et al., 2008) is located within an intramontane basin, 1 km SE of Lake Nam Co and in approximately 10 km distance NNW of the foot of the Nyainqentanglha mountain range. The zonal vegetation comprises mosaics of *Kobresia* turfs and open alpine steppe; water surplus sites have degraded Cyperaceae swamps (Mügler et al., 2010; Wei et al., 2012; Miehe et al., 2014).

2.2 Classification of the degradation classes at Kema site

The degradation classes were recorded at a defined area of 5 cm × 5 cm over a regular grid according to the step point method (Evans and Love, 1957), yielding a total of 2618 observations. The vegetation distribution is then calculated from the frequency of a given vegetation type vs. the total number of sampling points. Vegetation along each transect was classified according to the following classes (Fig. 2, Table 2): Intact root Mat (IM), Degraded root Mat (DM) and Bare Soil (BS).

Intact root Mat (IM)

Although this degradation class is named as IM in this study, according to the definition of Miehe et al. (2008b) it is already degraded. Closed *Kobresia* mats are normally char-

acterized as 90–98 % cover of *Kobresia pygmaea,* and additionally occurring biennial rosette species (Miehe et al., 2008b), which is not the case at Kema site. Nevertheless, soil is covered completely with the characteristic root turf of these Cyperaceae communities and a fairly closed cover of vegetation can be observed.

Degraded root Mat (DM)

For the DM class, not only is the spatial cover of *Kobresia pygmaea* much lower (less than 26 %), but also the proportion of crusts compared to IM is much higher; the root turf is still present. Crusts were formed by Cyanophyceae (blue algaea, Miehe et al., 2008b; Unteregelsbacher et al., 2012) and were a characteristic property of this classification.

Bare soil (BS)

In contrast to IM and DM, this surface class is missing the dense root turf and *Kobresia pygmaea* completely, resulting in a height step change (Table 2). Most of the surface is unvegetated, nevertheless annual and perennial plants still occur, e.g. *Lancea tibetica* and *Saussurea stoliczkai*, described as endemic biennial rosettes and endemic plants with rhizomes, adapted to soil movement and the occurrence of trampling (Miehe et al., 2011).

With a *Kobresia pygmaea* (Cyperaceae) cover of approximately 65 %, an area of 16 % crust-covered turf as well as 19 % bare soil spots, the main study site is considered to be a typical alpine *Kobresia pygmaea* pasture with a low to medium degradation state (Table 2).

2.3 Measuring methods

2.3.1 Micrometeorological measurements

The measurements of the water and carbon fluxes with the eddy-covariance (EC) method were conducted at Nam Co site in 2009 and at Kema site in 2010. The EC towers were equipped with CSAT3 sonic anemometers (Campbell Sci. Inc.) and LI-7500 (LI-COR Biosciences) gas analyzers. The complete instrumentation, including radiation and soil sensors, is given in Appendix A; for more details see Zhou et al. (2011) and Biermann et al. (2011, 2013).

Turbulent fluxes were calculated and quality controlled based on micrometeorological standards (Aubinet et al., 2012) through the application of the software package TK2/TK3 developed at the University of Bayreuth (Mauder and Foken, 2004, 2011). This includes all necessary data correction and data quality tools (Foken et al., 2012a), was approved by comparison with six other commonly used software packages (Mauder et al., 2008) and successfully applied in numerous international field campaigns. It also offers a quality flagging system evaluating stationarity and development of turbulence (Foken and Wichura, 1996; Foken et al., 2004). Furthermore, a footprint analysis was performed (Göckede et al., 2004, 2006), which showed that the footprint area was within the classified land use type.

For the interpretation of the results, the so-called un-closure of the surface energy balance (Foken, 2008) with eddy-covariance data must be taken into account, especially when comparing eddy-covariance measurements with models that close the energy balance, like SEWAB (Kracher et al., 2009), or when comparing evapotranspiration sums with micro-lysimeter measurements. For Nam Co site Zhou et al. (2011) found that only 70 % of the available energy (net radiation minus ground heat flux) contributes to the sensible and latent heat flux, which is similar to the findings of other authors for the Tibetan Plateau (Tanaka et al., 2001; Yang et al., 2004). For the Nam Co 2009 data set we found a closure of 80 % while both eddy-covariance measurements in Kema 2010 showed a closure of 73 %. Following recent experimental studies,

we assume that the missing energy is to a large extent part of the sensible heat flux (Foken et al., 2011; Charuchittipan et al., 2014), which was also postulated from model studies (Ingwersen et al., 2011). We thus corrected the turbulent fluxes for the missing energy according to the percentage of sensible and latent heat flux contributing to the buoyancy flux following the suggestion of (Charuchittipan et al., 2014). This correction method attributes most of the residual to the sensible heat flux depending on the Bowen ratio; i.e. more than 90 % in case of Bo = 1, and roughly 60 % in case of Bo = 0.1. In contrast, eddy-covariance derived NEE fluxes were not corrected (Foken et al., 2012a).

2.3.2 Soil hydrological measurements

In order to directly assess hydrological properties of the different degradation stages we used small weighing micro-lysimeters as a well-established tool to monitor evapotranspiration, infiltration and volumetric soil water content (Wieser et al., 2008; van den Bergh et al., 2013). As it was necessary to allow for quick installation with minimum disturbance, we developed a technique based on near-natural monoliths extracted in transparent plexiglass tubes (diameter 15 cm, length 30 cm). The monoliths were visually examined for intactness of the soil structure and artificial water pathways along the sidewall and then reinserted in their natural place inside a protecting outer tube (inner diameter 15 cm).

A general problem with soil monoliths is the disruption of the flow paths to the lower soil horizons leading to artificially high water saturation in the lower part of the monolith (Ben-Gal and Shani, 2002; Gee et al., 2009). This was prevented by applying a constant suction with 10 hPa of a hanging water column maintained by a spread bundle of 20 glass wicks (2 mm diameter) leading through the bottom plate into a 10 cm long downward pipe (15 mm diameter). Drained water was collected in a 200 mL PE bottle.

Micro-lysimeters were set up in June 2010 on four subplots inside the fenced area of the Kema site at a distance of 20 to 50 m from the eddy covariance station. On each subplot one micro-lysimeter was installed in IM and one in BS at a maximum distance

of 1 m. All micro-lysimeters were weighed every 2 to 10 days with a precision hanging balance from 23 June to 5 September 2010 and from 2 June to 5 September 2012. Soil cores (3.3 cm diameter, 30 cm depth) were taken near every micro-lysimeter on 29 June 2010. The soil samples were weighed fresh and after drying in the laboratory at Lhasa. By relating the given water content to the weight of the corresponding micro-lysimeter at that date, we were able to calculate volumetric soil water content for each micro-lysimeter over the whole measuring period.

2.3.3 Soil gas exchange measurements

In 2012, CO_2 flux measurements were conducted with a long-term chamber system from LI-COR Biosciences (Lincoln, NE, USA). This LI-COR long term chamber system contains a LI-8100 Infrared Gas Analyser (LI-COR Lincoln, NE, USA), is linked with an automated multiplexing system (LI-8150) and two automated chambers, one opaque and the other transparent for R_{eco} and net ecosystem exchange (NEE), respectively. The chambers are equipped with a fully automatically rotating arm that moves the chamber 180° away from the collar and therefore ensures undisturbed patterns of precipitation, temperature and radiation. Furthermore, by moving the chamber in-between measurements the soil and vegetation itself experiences less disturbance. The applied LI-COR chambers were compared during a separate experiment against eddy-covariance measurements by Riederer et al. (2014). Besides differences – mainly under stable atmospheric stratification – the comparison was satisfactory. For daily sums, the reported differences should compensate.

The three surface types IM, DM and BS were investigated with respect to their CO_2 fluxes between 30 July and 26 August 2012 at Kema. The CO_2-flux measurements of the three treatments were conducted consecutively. Therefore, the long–term chambers were moved to a patch representing the surface of interest. Measurements were conducted for five to nine days before rotating to another location, starting from IM (30 July–7 August), continuing at BS (7–15 August), DM (15–21 August) and ending again at IM (21–26 August).

Intact root mat has been measured twice during the observation period to provide information about possible changes in the magnitude of CO_2-fluxes, due to changing meteorological parameters. The two measurements will be denoted as IM period 1 and IM period 4. Note that during the measurement of IM period 4, other collars than during IM period 1 have been investigated. Nevertheless, the patches selected for the collar installation consisted of the same plant community, and showed the same soil characteristics. Because of lack of time the other two surfaces BS and DM were only measured once, but as long as possible to gather sufficient information on diurnal cycles for these treatments.

2.3.4 ^{13}C labeling

$^{13}CO_2$ pulse labeling experiments were used to trace allocation of assimilated C in the shoot–root–soil system in a montane *Kobresia pygmaea* pasture 2009 in Xinghai (Hafner et al., 2012) and in alpine *Kobresia pygmaea* pasture 2010 in Kema (Ingrisch et al., 2014). Plots ($0.6 \times 0.6\,m^2$) with plants were labelled with ^{13}C-enriched CO_2 in transparent chambers over four hours at the periods of maximal *Kobresia* growth in summer. Afterwards, ^{13}C was chased in the plant–soil system over a period of 2 months with increasing sampling intervals (10 times).

Aboveground biomass was clipped and belowground pools were sampled with a soil core (0–5, 5–15 cm and in Xinghai additionally in 15–30 cm). After drying and sieving (2 mm), two belowground pools were separated into soil and roots. As the only means of obtaining measurements of soil CO_2 efflux and its $\delta^{13}C$ in a remote location, the static alkali absorption method with installation of NaOH-traps was used (Lundegardh, 1921; Singh and Gupta, 1977; Hafner et al., 2012). Natural ^{13}C abundance in the pools of plant–soil systems, including CO_2 efflux, was sampled with a similar procedure on unlabelled spots. Total carbon and nitrogen content and $\delta^{13}C$ of the samples were analysed with an Isotope-Ratio Mass Spectrometer. All details of the $^{13}CO_2$ pulse labelling experiments were described in Hafner et al. (2012) and Ingrisch et al. (2014).

All data from ^{13}C labelling experiments are presented as means ± standard errors. The significance of differences was analyzed by ANOVA at $\alpha = 0.05$.

2.4 Soil–vegetation–atmosphere transfer models

We conducted model experiments in order to estimate the impact of the defined degradation classes on water and carbon fluxes, including feedback on atmospheric circulation. Therefore three 1-D soil–vegetation–atmosphere transfer models were utilized to examine, (i) evapotranspiration: SEWAB (Mengelkamp et al., 1999, 2001), (ii) carbon fluxes: SVAT-CN (Reichstein, 2001; Falge et al., 2005), (iii) surface feedbacks: hybrid vegetation dynamics and biosphere model (Friend et al., 1997; Friend and Kiang, 2005). While the first two models were driven by measured standard meteorological forcing data, the latter is fully coupled to the atmosphere with the cloud-resolving Active Tracer High-resolution Atmospheric Model (ATHAM, Oberhuber et al., 1998; Herzog et al., 2003), which allows for feedbacks of land surface exchange to the atmosphere (see Appendices B and C for more detailed descriptions of the models).

Land surface modelling of energy and carbon dioxide exchange faces specific problems on the Tibetan Plateau due to its high elevation and semi-arid conditions: a strong diurnal cycle of the surface temperature (Yang et al., 2009; Hong et al., 2010), a diurnal variation of the thermal roughness length observed on the Tibetan Plateau (Ma et al., 2002; Yang et al., 2003), and high bare soil evaporation in semiarid areas (e.g. Agam et al., 2004; Balsamo et al., 2011).

Especially the *Kobresia* mats are characterised by changing fractions of vegetation cover and partly missing root mats, exposing almost bare soil with properties different from the turf below the *Kobresia*. The models have therefore been adapted to these conditions and specific parameter sets have been elaborated from field measurements for Nam Co and Kema (Gerken et al., 2012; Biermann et al., 2014)

2.5 Experimental and modelling concept

Experimental investigations on the Tibetan Plateau are not comparable with typical meteorological and ecological experiments. Not only do the high altitude and the remote area impose limitations, but also unforeseeable administrative regulations challenge the organization of experiments with different groups and large equipment. It was initially planned to investigate small degraded plots with chambers and micro-lysimeters and to use a larger plot, in the size of the eddy-covariance footprint, as a reference area to investigate the daily fluctuations of the evaporation and carbon dioxide flux. Due to customs and permit problems, this was unfortunately only partly possible at Kema site in 2010, but not during the main chamber experiment in 2012. Therefore, model-specific parameters were investigated in 2012 and the models were adapted to the specific Tibetan conditions with the chamber data. These model versions were then tested with the eddy-covariance data in 2010 at Kema site with nearly intact *Kobresia* cover. A summary of the experimental setup according to measurement technique is given in Table 3.

In accordance with this concept, we adapted both SEWAB and SVAT-CN to the Kema site using the vegetation and soil parameters elaborated in 2012, and chamber measurements from 2012 for calibration. Two parameter sets were established: one for surfaces with root mat (Kema RM: IM and DM differ only in vegetation fraction), and one for BS conditions (Kema BS). Simulations with in situ measured atmospheric forcing data were performed specifically for each of the degradation classes S_{IM}, S_{DM} and S_{BS} according to the definition in Table 2. These model runs serve to expand the chamber data beyond their measurement period, and we are now able to compare the class-specific fluxes over a 46 day period (12 July to 26 August 2012).

Furthermore, we compared the adapted model versions with eddy-covariance data from 2010 using the respective forcing data measured in-situ in 2010. The eddy-covariance measurements integrate the fluxes from a source area ranging from 50–200 m around the instrument (for detailed footprint analysis see Biermann et al., 2011,

2013), and therefore represent H_2O and CO_2 fluxes from IM, DM and BS according to their proportion of total surface area in Table 2. In order to ensure comparability we reproduce this composition with the simulations as well using the tile approach (S_{RefEC}). An overview of model scenarios conducted at Kema site is given in Table 4.

For the investigation of the atmospheric impact of surface degradation, it was decided to run a relatively simple numerical experiment prescribing a symmetric, two-dimensional Tibetan valley with 150 km width, and surrounded by Gaussian hills with 1000 m altitude. A sounding taken at Nam Co at 17 July 2012 was used as the initial profile. The setup is comparable to Gerken et al. (2013, 2014). A total of four cases were chosen for this preliminary analysis. A dry scenario with initial soil moisture of 0.5× field capacity and a wet scenario with soil moisture at field capacity, as might be the case during the monsoon season, were used. For both surface states, simulations were performed with a vegetation cover of 25 % and 75 % corresponding to a degraded and intact soil-mat scenario.

The study is limited by conceptual restrictions mainly due to the scale problem in the different compartments (Foken et al., 2012b, see Appendix of this paper) and the working conditions in remote and high altitudes. Only one more-or-less uniform type of degradation has been investigated within the footprint area of the eddy-covariance measurements (Göckede et al., 2006) up to 50–200 m extension, which is, in the case of this study, an almost non-degraded *Kobresia* pasture. The other types could only be found on much smaller plots, and had no significant influence on the whole footprint area, even when considering the non-linear influence of the different land-cover areas on the fluxes of the larger area (Mölders, 2012). However, the investigation of degraded stages could only be done with small-scale measurements like chambers and micro-lysimeters.

3 Results and discussion

3.1 Comparison of measured and modelled fluxes

In order to test the performance of evapotranspiration (ET) with SEWAB and net ecosystem exchange (NEE) with SVAT-CN, we compared the model results for Kema with the eddy-covariance measurements from 2010 (Sect. 2.5). The results show that SEWAB simulations represent the half-hourly measured turbulent fluxes at Kema generally well ($y = 1.03x - 0.28\,\mathrm{mm\,d^{-1}}$, $r^2 = 0.72$, $n = 577$, Appendix D). Therefore, the simulations are well suited to filling the gaps in the eddy-covariance measurements for comparison of evapotranspiration with micro-lysimeter measurements. Model performance at Nam Co for the measurements in 2009 was very similar, as well as the magnitude of the fluxes (Biermann et al., 2014). Measured hourly medians of NEE at Kema ranged between −2.8 and $1.5\,\mathrm{g\,C\,m^{-2}\,d^{-1}}$ over the course of the day, whereas modelled medians reached a minimum −3.0 and a maximum of $1.7\,\mathrm{g\,C\,m^{-2}\,d^{-1}}$. Although the model overestimated the CO_2 uptake, especially in the midday hours, the correlation between hourly medians of model output and measured NEE was generally realistic ($y = 0.99x - 0.02\,\mathrm{g\,C\,m^{-2}\,d^{-1}}$, $r^2 = 0.81$, $n = 24$). Compared to Kema data, mean diurnal patterns of measured and modelled NEE showed smaller fluxes and less variation. Measured hourly medians of NEE ranged between −2.3 and $1.0\,\mathrm{g\,C\,m^{-2}\,d^{-1}}$ over the course of the day, and modelled medians between −2.7 and $1.0\,\mathrm{g\,C\,m^{-2}\,d^{-1}}$ ($y = 1.15x - 0.15\,\mathrm{g\,C\,m^{-2}\,d^{-1}}$, $r^2 = 0.9$, $n = 24$).

3.2 Evapotranspiration: EC – Micro-Lysimeter – SEWAB

Daily evapotranspiration (ET) of the *Kobresia pygmaea* ecosystem was about $2\,\mathrm{mm\,d^{-1}}$ during dry periods and increased to $6\,\mathrm{mm\,d^{-1}}$ after sufficient precipitation (not shown). This was confirmed with three different approaches: small weighable micro-lysimeters giving a direct measure of ET from small soil columns over several days, eddy-covariance measurements, but representing a larger area of ca. 150 m radius, and

SEWAB simulations. For a 33 day period at Kema 2010, ET for both micro-lysimeter and simulations varied around 1.9 mm d^{-1}, reflecting drier conditions, while in 2012 the micro-lysimeter showed a maximum ET of 2.7 mm d^{-1} at BS, and the simulations 3.5 mm d^{-1} at IM (Fig. 3). In summary, all approaches showed no clear differences between ET from IM and BS spots. Even for dense vegetation cover (IM), a considerable part of ET stems from evaporation. At DM and BS, transpiration of the small aboveground part of *Kobresia* is decreasing, but it is compensated by evaporation. Therefore, the water balance is mainly driven by physical factors, i.e. atmospheric evaporative demand and soil water content.

3.3 Carbon flux: chamber – SVAT-CN

During the Kema 2012 campaign the carbon fluxes for different degradation levels were investigated with chamber-based gas exchange measurements. Parallel measurements could not be established due to instrumental limitations, therefore the SVAT-CN model is utilised to compare the degradation classes over the whole period. In order to adapt SVAT-CN to the chamber measurements, the parameters of leaf physiology and soil respiration have been set to values that accommodate the different vegetation types and cover of the plots (Appendix C, Table C2).

Daily sums of ecosystem respiration (R_{eco}) over IM were overestimated by the model during period 1, but underestimated during the second setup over IM (period 4); see Fig. 4. Overall, the model predicted a mean R_{eco} of 2.37 g C m^{-2} d^{-1} for IM, whereas the mean of the chamber data yield 2.31 g C m^{-2} d^{-1}. For the chamber setup over bare soil (BS, period 2), R_{eco} were, on average, represented well by the model (on average 0.77 g C m^{-2} s^{-1}) as compared to the data average of 0.81 g C m^{-2} d^{-1}. Similarly, for DM (period 3) modelled (1.81 g C m^{-2} d^{-1}) and measured (1.69 g C m^{-2} d^{-1}) average R_{eco} compared well. Analogous patterns were found for daily sums of gross ecosystem exchange (GEE = NEE$-R_{eco}$): under- and overestimations of the daily sums characterized the setups over IM (period 1 and 4), but were compensated to some extent when

analyzing period 1 and 4 together (modelled average GEE −5.39 g C m^{-2} d^{-1}, measured average GEE −4.96 g C m^{-2} s^{-1}). Average modelled GEE over BS with −0.89 g C m^{-2} d^{-1} compared well to measured GEE for period 2 (−0.69 g C m^{-2} d^{-1}). Over DM, the average modelled GEE was −1.64 g C m^{-2} d^{-1}, and measured GEE showed an average of −1.94 g C m^{-2} d^{-1}.

The mean carbon fluxes derived from SVAT-CN simulations for the different degradation classes over the vegetation period are shown in Fig. 5. A noticeable carbon uptake of −2.89 g C m^{-2} d^{-1} for IM reduces to −0.09 for BS and even shifts to a weak release of 0.2 at DM. This is mainly related to a drop in GEE by 83 % for BS and 64 % for DM, compared to IM (100 %). While Reco for BS is reduced by 66 %, it only reduces by 12 % for DM, leading to the small net release already mentioned.

Cumulative NEE was calculated applying the four different model setups previously described: IM, DM and BS stages of *Kobresia* pastures at Kema, and Alpine Steppe (AS) ecosystem at Nam Co (Fig. 6). The simulation period ranged from period 12 July to 26 August 2012. For this period, only the IM stage showed significant carbon uptake of −133 g C m^{-2}. DM and BS ecosystems were more-or-less carbon neutral (−4 g C m^{-2} uptake at BS, and 9 g C m^{-2} release at DM). The model for AS resulted in a carbon loss of 24 g C m^{-2} for the investigated period.

3.4 Distribution of the assimilated carbon in *Kobresia* pastures and the soil

The results from two $^{13}CO_2$ pulse labelling experiments at Xinghai 2009 (Hafner et al., 2012) and Kema 2010 (Ingrisch et al., 2014) show the distribution of assimilated carbon (C) in a montane and alpine *Kobresia* pasture (Fig. 7). The study in Xinghai showed that C translocation was different on plots where vegetation had changed from Cyperaceae to Poaceae dominance, induced by grazing cessation. Less assimilated C was stored in belowground pools. The study in Kema showed that roots within the turf layer act as the main sink for recently assimilated C (65 %) and as the most dynamic part of the ecosystem in terms of C turnover. This is also the main difference between the

experiments on the two sites as in the case of the alpine pasture (Kema) more C was allocated belowground than in montane pasture. However, as the experiments were conducted under different conditions and in consecutive years, a comparison of absolute values is not possible as the determined C fraction varies also throughout the growing season (Swinnen et al., 1994; Kuzyakov and Domanski, 2000).

At Kema, the $^{13}CO_2$ labelling was furthermore coupled with eddy-covariance measurements to determine absolute values of the carbon distribution in the plants, roots and the soil following a method developed by Riederer (2014). In addition, the continuous observation of the exchange regime with the EC confirms that the pulse labelling was conducted under atmospheric conditions similar to the ones of the whole allocation period. This leads to more representativeness of the result of the $^{13}CO_2$ labelling experiment, which could not be repeated due to the remote and restricted access on the Plateau.

3.5 Influence of plant cover on convection and precipitation

For investigating the influence of degradation on the development of convection and precipitation, the ATHAM model was applied for 25 % (V25) and 75 % (V75) plant cover at the Nam Co basin, with each of these in a dry and a wet scenario. From Fig. 8 it becomes immediately apparent that wet surface conditions are associated with higher deposited precipitation. At the same time, near-surface relative humidities are higher (not shown). For both the dry and wet cases an earlier cloud and convection development is observed for the less vegetated surface: simulations produce higher cloud cover and more convection from 10:00 local solar time (LST) onward. At Nam Co we observed the frequent development of locally generated convective systems at similar hours in the field. Thus clouds block more incoming solar radiation between 10:00 and 14:00 LST, the time with the potentially highest shortwave radiation forcing, for the less vegetated system compared to the intact vegetation scenario. Consequently, simulated surface temperatures were higher for the V75 scenario, leading to higher surface fluxes and a stronger simulated convection development over the day as a whole. A potential

albedo effect can be excluded since the observed albedo of the vegetated surface is similar to that of the bare surface and surface temperatures remain virtually identical until convection develops.

The mechanism for this process is presumably that the vegetation cover reduces bare soil evaporation. At the same time, higher surface temperatures due to higher radiation input result in both larger sensible and latent heat fluxes in the afternoon hours, while the plant cover is able to access water that is not available for surface evaporation.

This hypothesis obviously needs to be investigated more thoroughly with field observations and simulations, but the findings indicate that changes in surface conditions can affect convective dynamics and local weather. This preliminary investigation of vegetation–atmosphere feedbacks did not take into account any spatial patterns in surface degradation that may result in larger patches with different surface conditions that may then affect circulation. However, such circulation effects are typically found in modelling studies using patch sizes with length scales that are several times the boundary-layer height.

3.6 Simulation of different degradation states

The results for the different degradation states allow the simulation of the NEE and evapotranspiration for a gradual change from IM to BS using a tile approach of the fluxes (Avissar and Pielke, 1989). Such a tile approach is exemplarily shown for different percentages of the ecosystem types IM and BS for a 46 days period in July and August 2012 at Kema site, with simulated NEE (Fig. 9a) and evapotranspiration (Fig. 9b). As expected from the cumulative carbon gains for S_{IM} and S_{BS} shown in Fig. 5, S_{IM} developed the largest carbon sink over the investigated summer period, whereas S_{BS} is nearly carbon neutral in summer and a source for longer periods. The intermediate stages showed decreasing average carbon uptake with increasing amount of bare soil. Diurnal variability is largest for 100 % S_{IM} and smallest for 100 % S_{BS} in the ecosystem,

as indicated by the interquartile ranges in the box plot. The related mean diurnal cycles are given in Appendix B, Fig. B1.

Evapotranspiration decreases from S_{IM} to S_{BS} in this model degradation experiment, while the day-to-day variability increases (Fig. 9b). This is connected to a larger variability of simulated soil moisture in the uppermost layer, as the turf layer retains more water due to its higher field capacity and lower soil hydraulic conductivity, and the roots can extract water for transpiration from lower soil layers as well.

4 Conclusions

The approach to the investigation of the three prevailing degradation stages, Intact root Mat (IM), Degraded root Mat (DM) and Bare Soil (BS), opened new insights and perspectives, using and integrating chamber measurements, micro-lysimeter, eddy-covariance measurements, and model studies.

Increasing degradation of the *Kobresia pygmaea* turf significantly reduces the carbon uptake and the function of *Kobresia* pastures as a carbon sink, while the influence on the evapotranspiration is less dominant. However, the shift from transpiration to evaporation was found to have a significant influence on the starting time of convection and cloud and precipitation generation: convection starts above a degraded surface around noon instead of later in the afternoon. Due to the dominant direct solar radiation on the Tibetan Plateau, the early-generated cloud cover reduces the energy input and therefore the surface temperatures. Therefore the degradation state of the *Kobresia* pastures has a significant influence on the water and carbon cycle and, in consequence, on the climate system. Due to the relevance of the Tibetan Plateau on the global circulation changes, the surface properties on the highland have influences on larger scales. These changes in the water and carbon cycle are furthermore influenced by global warming and an extended growing season (Che et al., 2014; Shen et al., 2014; Zhang et al., 2014).

Plot size experiments are a promising mechanistic tool for investigating processes that are relevant for larger scales. Since all results showed a high correlation between modelled and experimental data, a combination is possible with a tile approach with flux averaging to realize model studies that consider gradual degradation schemata. The consequent combination of plot scale, ecosystem scale and landscape scale shows the importance of the integration of experimental and modelling approaches.

The palaeo-environmental reconstruction (Miehe et al., 2014) as well as the simulations of the present study suggest that the present grazing lawns of *Kobresia pygmaea* are a synanthropic ecosystem that developed through long-lasting selective free-range grazing of livestock. This traditional and obviously sustainable rangeland management would be the best way to conserve and possibly increase the carbon stocks in the turf and its functions. Otherwise, an overgrazing connected with erosion would destroy the carbon sink. Considering the large area, even the loss of this small sink would have an influence on the climate relevant carbon balance of China.

From our investigation we propose the need for the following additional research.

- Extension of this integrated experimental-modelling research scheme to the full annual cycle.
- The results obtained so far on just these three sites should be extended to an increased number of experimental sites, supported by appropriate remote sensing tools, in order to regionalize degradation patterns and related processes.
- Investigation of the processes along elevation gradients, with special reference to functional dependences.
- The use of remote sensing cloud cover studies to evaluate simulations of cloud generation and precipitation depending on surface structures.

Appendix A: Instrumentation of the measurement sites

The instrumentation of the measurement sites is given for Kema in Table A1 and for Nam Co in Table A2.

Appendix B: Soil–vegetation–atmosphere transfer models

Land surface modelling of energy and carbon dioxide exchange faces specific problems on the Tibetan Plateau. Most influential is the strong diurnal cycle of the surface temperature, observed in dry conditions over bare soil or very low vegetation, leading to overestimation of surface sensible heat flux (Yang et al., 2009; Hong et al., 2010) caused by too high turbulent diffusion coefficients. Land surface models usually parameterize these coefficients by a fixed fraction between the roughness length of momentum and heat, however, Yang et al. (2003) and Ma et al. (2002) observed a diurnal variation of the thermal roughness length on the Tibetan Plateau. As another special feature, land surface models tend to underestimate bare soil evaporation in semiarid areas (e.g. Agam et al., 2004; Balsamo et al., 2011); even for soil moisture below wilting point some evaporation could be observed.

Especially the *Kobresia pygmaea* mats are characterised by changing fractions of vegetation cover and partly missing root mats, exposing almost bare soil with properties different from the turf below the *Kobresia pygmaea*. From investigations of soil vertical heterogeneity by Yang et al. (2005) it can be concluded that such variations will significantly influence the exchange processes, posing a challenge for land surface modelling.

B1 Evapotranspiration – the SEWAB model

To model the sensible and latent heat flux at Kema site the 1-D soil–vegetation–atmosphere transfer scheme SEWAB (Surface Energy and WAter Balance model) was applied (Mengelkamp et al., 1999, 2001). The soil temperature distribution is solved

by the diffusion equation and vertical movement of soil water is described by the Richards equation (Richards, 1931). Relationships between soil moisture characteristics are given by Clapp and Hornberger (1978). Atmospheric exchange is given by bulk approaches, taking into account aerodynamic and thermal roughness lengths with respect to atmospheric stability (Louis, 1979). The latent heat flux is split up into vegetated surface flux and bare soil evaporation. The flux from vegetation is composed of wet foliage evaporation and transpiration of dry leaves. For the latter, the stomata resistance is constrained by minimum resistance and stress factors in a Jarvis-type scheme (Noilhan and Planton, 1989). In contrast to many other SVAT models, SEWAB parameterizes all energy balance components separately and closes the energy balance by an iteration for the surface temperature using Brent's method.

B2 Carbon dioxide exchange – the SVAT-CN

The model SVAT-CN (Reichstein, 2001; Falge et al., 2005) simulates CO_2 and H_2O gas exchange of vegetation and soil. It consists of a 1-D canopy model (Caldwell et al., 1986; Tenhunen et al., 1995), a 1-D soil physical model of water and heat fluxes (Moldrup et al., 1989, 1991), and a model of root water uptake (Reichstein, 2001). The model has been further developed with respect to soil gas emissions of CO_2 and N_2O from forest, grassland, and fallow (Reth et al., 2005a, b, c). In combination with a 3-D model it has been used to simulate vertical profiles of latent heat exchange and successfully compared to vertical profiles of latent heat exchange in a spruce forest canopy (Staudt et al., 2011; Foken et al., 2012b). Plant canopy and soil are represented by several horizontally homogeneous layers, for which microclimate and gas exchange is computed. The soil module simulates unsaturated water flow according to Richards equation (Richards, 1931) parameterized with van Genuchten (1980) soil hydraulic parameters. C_3 photosynthesis is modelled using the basic formulation described by Farquhar et al. (1980). Stomatal conductance is linked linearly to assimilation and environmental controls via the Ball–Berry equation (Ball et al., 1987). The slope of this

equation (gfac) is modelled depending on soil matrix potential (Ψ) in the main root layer.

B3 2-D atmospheric model – ATHAM

In a separate work (Gerken et al., 2012), the SEWAB model compared well with the Hybrid vegetation dynamics and biosphere model (Friend et al., 1997; Friend and Kiang, 2005)), which is coupled to the cloud-resolving Active Tracer High-resolution Atmospheric Model (ATHAM, Oberhuber et al., 1998; Herzog et al., 2003). The fully coupled system was successful in simulating surface–atmosphere interactions, mesoscale circulations and convective evolution in the Nam Co basin (Gerken et al., 2013, 2014). In a coupled simulation, surface fluxes of energy and moisture interact with the flow field. At the same time, wind speed as well as clouds, which modify the surface radiation-balance, provide a feedback to the surface and modify turbulent fluxes. Such simulations can produce a complex system of interactions.

Appendix C: Model adaption to the Tibetan Plateau

C1 Adaption of SEWAB

Considering the specific problems on the Tibetan Plateau, three changes have been implemented in SEWAB. Those are a variable thermal roughness length (Yang et al., 2008), soil thermal conductivity calculation (Yang et al., 2005) and the parameterization of bare soil evaporation (Mihailovic et al., 1993). These changes have been already applied and evaluated at the alpine steppe site Nam Co using the same data set (Gerken et al., 2012; Biermann et al., 2014)

Furthermore, all relevant model parameters have been adapted to the site-specific conditions (see Table C1). The parameters for the alpine steppe site Nam Co have been used as published in Biermann et al. (2014), which were inferred from field and

laboratory measurements. Specific parameters for the Kema site have been elaborated as follows: albedo has been estimated from radiation measurements individually for the 2010 and 2012 data set. The fraction of vegetated area has been surveyed (Sect. 2.2), root depth is assessed from soil profiles (Biermann et al., 2011, 2013) and the roughness length for momentum is estimated from eddy-covariance friction velocity under neutral conditions. The LAI for the vegetated area has been calculated from a biomass survey (September 2012, $n = 5$) and subsequent scans of leaf surface using WinSeedle. Maximum stomatal conductance has been elaborated by gas exchange measurements with *Kobresia pygmaea* in Göttingen (see Appendix C2), which has been translated to minimum stomatal resistance.

Soil properties have been estimated from measurements separately for conditions with root mat (RM: IM and DM) and without root mat (BS). As SEWAB accepts only one soil parameter set for the whole soil column, the properties of the uppermost 5 cm have been used. The bulk density has been surveyed in 2012 for soil layers of 5 cm thickness, down to 30 cm for RM and 14 cm for BS ($n = 4$ plots $\times 4$ replicates $= 16$ for each layer). Average soil organic carbon content of the turf layer was 9 %, measured by dry combustion (Vario EL, Elementar, Hanau), corresponding to approximately 18 % organic matter, which is in agreement with previous analyses by Kaiser et al. (2008). This amount has been distributed to three layers of 5 cm according to the relative content of root mass in each layer, sampled in 2010 ($n = 4$ plots $\times 3$ replicates $= 12$ for each layer). From bulk density and mass fraction of organic matter the porosity in 0–5 cm depth is estimated with $0.593\,m^3\,m^{-3}$, assuming densities of $2.65\,g\,m^{-3}$ for mineral content and $1.2\,g\,m^{-3}$ for organic content. The soil heat capacity of solid matter is combined from $2.1 \times 10^6\,J\,m^{-3}\,K^{-1}$ for mineral content and $2.5 \times 10^6\,J\,m^{-3}\,K^{-1}$ for organic matter according to Hillel (1980). Thermal conductivities for dry soil and at saturation, needed for the conductivity calculation (Yang et al., 2005), have been investigated for a similar turf layer (Chen et al., 2012: Anduo site for RM, BJ site for BS). Further, we derived saturated hydraulic conductivities of $1.9 \times 10^{-5}\,m\,s^{-1}$ and $4.6 \times 10^{-5}\,m\,s^{-1}$ as mean values for RM and BS, respectively, using infiltrometer measurements from

2010 (Biermann et al., 2011, 2013). An in-situ soil water retention curve was established from tensiometer and TDR profile measurements in 2012, reflecting the properties of RM in the first 15 cm and the properties of BS in 25 cm depth. From this data the matrix potential at saturation Ψ_{sat} and the exponent b for the relationship by Clapp and Hornberger (1978) is estimated via linear regression of the logarithmic form: $\log(\Psi_\Theta) = \log(\Psi_{sat}) + b \cdot \log(\frac{\Theta_{sat}}{\Theta})$. Further, the soil water content at field capacity and wilting point has been derived from this relationship assuming pF values (= $\log(\Psi_\Theta)$) of 2.5 log(hPa) and 4.5 log(hPa) for Θ_{FC} and Θ_{WP}, respectively.

C2 Adaption of SVAT-CN

Species parameterization of the leaf model for *Kobresia pygmaea*:

Measurements of in situ CO_2 and H_2O leaf gas exchange in response to temperature, radiation, CO_2 mixing ratio, and relative humidity were made using a portable gas exchange system (WALZ GFS3000, Walz, Effeltrich/Germany). Single factor dependencies of leaf gas exchange to light, temperature, CO_2 mixing ratio, and relative humidity, were performed for copiously watered *Kobresia pygmaea* plants from greenhouse experiments at the University of Göttingen. The measurement setup was situated in a greenhouse chamber regulated to 15 °C. GFS3000 gas exchange measurements were performed at six different temperatures (7.5, 10, 15, 20, 25, and 30 °C) inside the cuvette and a series of different relative humidities of the inlet air, ranging between 20 and 65 %, matching meteorological conditions found at the field site during the intensive campaign in 2010. As high humidity inside the chamber system leads to problems with water condensation in the tubes, the conditions were restricted to relative humidity up to 65 %. Data have been analyzed using with the physiologically based leaf gas exchange model (Farquhar et al., 1980; Ball et al., 1987) to derive estimates for those parameters that describe the carboxylase kinetics, electron transport, respiration and stomatal function. We used a non-linear least trimmed squares regression tool (Reth et al., 2005c), that minimizes the sum of squared residuals excluding the largest 5 % of

residuals, assumed to indicate data contamination or data-model inconsistencies. Sets of parameter values for *Kobresia pygmaea* (Appendix, Table C2) were obtained as the basis for calculating canopy flux rates at the different field sites.

Parameterization of soil retention curve:

In SVAT-CN the relationship between soil matrix potential Ψ (or better water suction, in units of m) and soil water content θ ($m^3\,m^{-3}$) is described by a retention curve after van Genuchten (1980)

$$\Psi(\theta) = \frac{1}{\alpha} \cdot \left[\left(\frac{\theta - \theta_r}{\theta_s - \theta_r} \right)^{-\frac{1}{m}} - 1 \right]^{\frac{1}{n}}, \quad \text{(C1)}$$

where θ is soil water content ($m^3\,m^{-3}$), θ_r soil residual water content ($m^3\,m^{-3}$), θ_s soil saturated water content ($m^3\,m^{-3}$), α a scale parameter (m^{-1}), and n and m shape parameters, with $m = 1–1/n$. Site-specific data of measured retention curves (soil moisture and soil water potential from AWS, Table A1) have been used to parameterize θ_r, α, and n (Appendix, Table C1) by non-linear least square regression.

Parameterization of soil respiration:

Soil respiration (R_s, $\mu mol\,m^{-2}\,s^{-1}$) is modelled as a function of modelled soil temperature T_s (K) and soil water content θ ($m^3\,m^{-3}$) in 10 cm depth as follows:

$$R_s = R_{norm} \cdot e^{\left(E_0 \cdot \frac{1}{T_{ref} - T_0} \cdot \frac{1}{T_s - T_0}\right)} \cdot \max\left(0.01, \frac{\theta - \theta_0}{(\theta_{half} - \theta_0) + (\theta - \theta_0)}\right) \quad \text{(C2)}$$

where R_{norm} is the base rate at optimum soil water content and reference temperature ($\mu mol\,m^{-2}\,s^{-1}$); E an activation energy parameter (°C) that determines temperature sensitivity; T_{ref} reference temperature (°C); T_0 (−46.02 °C, a regression parameter from

Lloyd and Taylor, 1994), θ the soil water content where the rate is reduced to zero ($m^3\,m^{-3}$), and θ_{half} the soil water content where the rate is reduced by half ($m^3\,m^{-3}$).

The original formulation in SVAT-CN was changed to accommodate the much higher soil organic content in the *Kobresia* ecosystems. T_{ref} and E were adapted to match soil respiration data measured with gas exchange chambers. For Kema a T_{ref} of 16 °C for the "*Kobresia*", and 24 °C for the "bare soil" plots, were used. At Nam Co T_{ref} was set to 16 °C. For all sites an E of 500 °C was employed. R_{norm} was 2.3 µmol $m^{-2}\,s^{-1}$. At all sites only weak dependences on soil water content were implemented, with θ set to θ_r of the retention parameterizations, and θ_{half} set to 0.035 $m^3\,m^{-3}$.

Parameterization of leaf gas exchange:

Species-specific parameters (Table C2) for the physiologically based leaf gas exchange model have been derived from CO_2 and H_2O leaf gas exchange measurements in the greenhouse (see "Species-specific parameterization of the leaf model for *Kobresia* pygmaea" in this section). For the simulation of the Kema campaign in 2012, at first the original parameters of Table C2 were used for the vegetated area of the different degradation states of "*Kobresia*" (IM and DM) and "bare soil" plots, but underestimated the measured chamber gas exchange data. Consequently, three scaling parameters $c(P_{ml})$, $c(Vc_{max})$, and $F(R_d)$ were increased to 160 % of the original values (Appendix, Table C2) for better comparison with measured data. The same parameters were used for the Kema 2010 campaign. The slope of the linear equation, which links stomatal conductance to assimilation and environmental controls, is modelled depending on soil matrix potential (Ψ) in the main root layer: $gfac = \max(15, gfac_0 \times 10^{(0.025 \cdot \Psi)})$, Ψ in MPa, simulated in 10 cm depth. For the campaign in 2010 – a year with drought stress effects, the respective formulation was adapted to $gfac = \max(5, gfac_0 \times 10^{(0.1 \cdot \Psi)})$.

For Nam Co site, which is characterized by a vegetation composition of alpine steppe species different from the *Kobresia* pastures, no specific leaf gas exchange parameters are available. As a first attempt, leaf parameter sets of *Kobresia* were applied, but

these overestimated measured eddy covariance fluxes. Consecutive reduction of scaling parameters (Appendix, Table C2) yielded a better representation of the measured eddy covariance fluxes.

Appendix D: Model evaluation

D1 Evapotranspiration: EC – SEWAB

In order to test the performance of simulations of evapotranspiration with SEWAB, we compared the model results for Kema with the eddy-covariance measurements from 2010. Therefore the simulations for IM, DM and BS have been aggregated as weighted sums according to the eddy-covariance footprint (S_{RefEC}, see Table 4) and the measurements have been corrected according to the energy balance closure gap (Sect. 2.3.1). The results show that SEWAB simulations represent the measured evapotranspiration well (Fig. D1). Similarly, the simulations generally capture the diurnal cycle of evapotranspiration (Fig. D2), with median fluxes of approximately 6.5 mm d^{-1} at noon, and a large day-to-day variation caused by variable moisture conditions within the observation period in 2010. The simulations slightly overestimate daytime fluxes and underestimate nighttime fluxes, the overall bias with high quality flux data (flag 1–3 out of a scheme ranging from 1–9, Foken et al., 2004) is −0.13 mm d^{-1}. Therefore, the simulations are well suited to fill the gaps in the eddy-covariance measurements for comparison of evapotranspiration with micro-lysimeter measurements.

D2 Carbon flux: EC – SVAT-CN

Kema 2010 (IM):

For best representation of the eddy covariance data footprint, model results (S_{RefEC}, Table 5) are calculated as weighed sums of IM, DM and BS according to the proportion of total surface area in Table 2. Due to drier conditions in 2010, the vegetation was par-

tially considered to be photosynthetically inactive, therefore the LAI of vegetated area has been reduced from 1 to 0.5. Mean diurnal patterns of both, measured and modelled net ecosystem exchange showed CO_2 release during night, and uptake during daytime hours, with a pronounced peak in the late morning hours, and a smaller peak in the late afternoon (Fig. D3). However, measured hourly medians of net ecosystem exchange ranged between −2.8 and 1.5 g C m^{-2} d^{-1} over the course of the day, whereas modelled medians reached a minimum of −3.0 and a maximum of 1.7 g C m^{-2} d^{-1}.

Although the model overestimated the CO_2 uptake, especially in the midday hours, the correlation with r^2 of 0.81 between hourly medians of model output and measured NEE (Fig. D4, left) was generally realistic. The slope of the regression between predictions and measurements was 0.99, the offset −0.02 g C m^{-2} d^{-1}.

Nam Co 2009 (AS):

Compared to Kema data, mean diurnal patterns of measured and modelled net ecosystem exchange showed much smaller variation within a given hour (smaller interquartile ranges), and lower CO_2 release during night, and lower uptake during daytime hours (lower diurnal amplitudes, see Fig. D5). As leaf physiological parameters were adapted to match measurements and model results, the ranges of both measured and modelled medians showed a better overlap: measured hourly medians of net ecosystem exchange ranged between −2.3 and 1.0 g C m^{-2} d^{-1} over the course of the day, and modelled medians between −2.7 and 1.0 g C m^{-2} d^{-1}. The wide range of measured NEE from −6 g C m^{-2} d^{-1} to 1 g C m^{-2} d^{-1} at mid-day results from variable moisture conditions during the monsoon season and is consistent with chamber-based observations at a similar spot near Nam Co station (Hu et al., 2013).

At Nam Co the model overestimated the CO_2 uptake especially in the afternoon hours, indicating a larger influence of soil respiration than currently represented by the model. Simulated soil respiration depends on simulated driving variables (soil temperature and moisture) and parameters. The latter have not been measured at Nam Co directly; instead the values from Kema field site have been employed, eventually intro-

ducing the observed bias. Nevertheless, the correlation with r^2 of 0.90 between hourly medians of modelled and measured NEE (Fig. D4, right) was better than at Kema. The slope of the regression between predictions and measurements was 1.15, the offset −0.15 g C m^{-2} d^{-1}.

D3 Carbon flux: chamber – SVAT-CN

Using original leaf physiology scaled up to 160 % (see Appendix C2 and Table C2), net ecosystem exchange chamber data of period 1 (IM with LAI of 0.88) are slightly overestimated due to an offset of −0.95 (r^2 of 0.90, slope of 0.99). For period 2 (BS with LAI of 0.12), with very low flux rates, the model underestimates the NEE measurements with a slope of 1.77 and an offset of −0.38 (r^2 of 0.48). During period 3 (DM with LAI of 0.26), the model yields a realistic representation of the measured chamber fluxes with r^2 of 0.74, a slope of 0.85 and an offset of 0.24 g C m^{-2} d^{-1}. The linear regression parameters for period 4 (IM with LAI of 0.88) are r^2 of 0.89, slope of 0.69 and offset of −0.69 g C m^{-2} d^{-1}, underestimating the measured NEE.

Acknowledgements. The project was funded within the DFG (German Science Foundation) priority programme 1372 “Tibetan Plateau – Formation – Climate – Ecosystems (TiP)” with the contracts FO 226/18-1,2; GU 406/22-1,2; KU 1184/14-1,2; LE 762/12-1,2; MI 338/7-1,2; WE 2601/4-1,2. Special thanks for the additional funding of the modelling study with the contract AP 34/32-3. The Chinese scientists in the Institute of Tibetan Plateau Research, the Chinese Academy of Sciences were supported by the Chinese National Key Programme for Developing Basic Sciences with the contract 2010CB951701 and the National Natural Science Foundation of China with the contracts 91337212 and 41275010. The research station at Kema was supported by the Volkswagen foundation, in cooperation with the Marburg University and the Tibet University Lhasa, now managed by the Institute of Tibetan Plateau Research, (CAS) as “*Naqu Ecological and Environmental Observation and Research Station*”. All authors are very grateful to the staff of the research stations at Kema and Nam Co for their support. Furthermore, we thank LI-COR Biosciences for the lending of the chamber system and support. This publication is funded by the DFG and the University of Bayreuth in the funding programme Open Access Publishing.

References

Agam, N., Berliner, P. R., Zangvil, A., and Ben-Dor, E.: Soil water evaporation during the dry season in an arid zone, J. Geophys. Res., 109, D16103, doi:doi:10.1029/2004JD004802, 2004.

Aubinet, M., Vesala, T., and Papale, D.: Eddy Covariance: a Practical Guide to Measurement and Data Analysis, Springer, Dordrecht, Heidelberg, London, New York, 438 pp., 2012.

Avissar, R. and Pielke, R. A.: A parametrization of heterogeneous land surface for atmospheric numerical models and its impact on regional meteorology, Mon. Weather Rev., 117, 2113–2136, 1989.

Ball, J. T., Woodrow, I. E., and Berry, J. A.: A model predicting stomatal conductance and its contribution to the control of photosynthesis under different environmental conditions, in: Progress in Photosynthesis Research, Proceedings of the VII International Photosynthesis Congress, edited by: Binggins, I., 221–224, 1987.

Balsamo, G., Boussetta, S., Dutra, E., Beljaars, A., Viterbo, P., and van den Hurk, B.: Evolution of land surface processes in the IFS, ECMWF Newsletter, 127, 17–22, 2011.

Ben-Gal, A. and Shani, U.: A highly conductive drainage extension to control the lower boundary condition of lysimeters, Plant Soil, 239, 9–17, doi:10.1023/A:1014942024573, 2002.

Biermann, T., Leipold, T., Babel, W., Becker, L., Coners, H., Foken, T., Guggenberger, G., He, S., Ingrisch, J., Kuzyakov, Y., Leuschner, C., Miehe, G., Richards, K., Seeber, E., and Wesche, K.: Tibet Plateau Atmosphere–Ecology–Glaciology Cluster, Joint *Kobresia* Ecosystem Experiment: Documentation of the first Intensive Observation Period Summer 2010 in Kema, Tibet, Arbeitsergebn., Univ. Bayreuth, Abt. Mikrometeorol., ISSN 1614-8916, 44, 105, 2011.

Biermann, T., Seeber, E., Schleuß, P., Willinghöfer, S., Leonbacher, J., Schützenmeister, K., Steingräber, L., Babel, W., Coners, H., Foken, T., Guggenberger, G., Kuzyakov, Y., Leuschner, C., Miehe, G., and Wesche, K.: Tibet Plateau Atmosphere–Ecology–Glaciology Cluster Joint *Kobresia* Ecosystem Experiment: Documentation of the second Intensive Observation Period, Summer 2012 in KEMA, Tibet, Arbeitsergebn., Univ. Bayreuth, Abt. Mikrometeorol., ISSN 1614–8916, 54, 52, 2013.

Biermann, T., Babel, W., Ma, W., Chen, X., Thiem, E., Ma, Y., and Foken, T.: Turbulent flux observations and modelling over a shallow lake and a wet grassland in the Nam Co basin, Tibetan Plateau, Theor. Appl. Climatol., 116, 301–316, 2014.

Caldwell, M. M., Meister, H. P., Tenhunen, J. D., and Lange, O. L.: Canopy structure, light microclimate and leaf gas exchange of *Quercus coccifera* L. in a Portugese macchia: measurements in different canopy layers and simulations with a canopy model, Trees, 1, 25–41, 1986.

Charuchittipan, D., Babel, W., Mauder, M., Leps, J.-P., and Foken, T.: Extension of the averaging time of the eddy-covariance measurement and its effect on the energy balance closure Bound.-Lay. Meteorol., online first, doi:10.1007/s10546-014-9922-6, 2014.

Che, M., Chen, B., Innes, J. L., Wang, G., Dou, X., Zhou, T., Zhang, H., Yan, J., Xu, G., and Zhao, H.: Spatial and temporal variations in the end date of the vegetation growing season throughout the Qinghai–Tibetan Plateau from 1982 to 2011, Agr. Forest Meteorol., 189–190, 81–90, doi:10.1016/j.agrformet.2014.01.004, 2014.

Chen, Y., Yang, K., Tang, W., Qin, J., and Zhao, L.: Parameterizing soil organic carbon's impacts on soil porosity and thermal parameters for Eastern Tibet grasslands, Sci. China Ser. D, 55, 1001–1011, 2012.

Clapp, R. B. and Hornberger, G. M.: Empirical equations for some soil hydraulic properties, Water Resour. Res., 14, 601–604, 1978.

Cui, X. and Graf, H.-F.: Recent land cover changes on the Tibetan Plateau: a review, Climatic Change, 94, 47–61, doi:10.1007/s10584-009-9556-8, 2009.

Evans, R. A. and Love, R. M.: The step-point method of sampling – a practical tool in range research, J. Range Manage., 10, 208–212, 1957.

Falge, E.: Die Modellierung der Kronendachtranspiration von Fichtenbeständen (*Picea abies* (L.) Karst., Bayreuther Forum Ökologie, 48, XX, 1997.

Falge, E., Reth, S., Brüggemann, N., Butterbach-Bahl, K., Goldberg, V., Oltchev, A., Schaaf, S., Spindler, G., Stiller, B., Queck, R., Köstner, B., and Bernhofer, C.: Comparison of surface energy exchange models with eddy flux data in forest and grassland ecosystems of Germany, Ecol. Model., 188, 174–216, 2005.

Farquhar, G. D., von Caemmerer, S., and Berry, J. A.: A biochemical of photosynthetic CO_2 assimilation in leaves of C_3 species, Planta, 149, 78–90, 1980.

Foken, T.: The energy balance closure problem – an overview, Ecol. Appl., 18, 1351–1367, 2008.

Foken, T. and Wichura, B.: Tools for quality assessment of surface-based flux measurements, Agr. Forest Meteorol., 78, 83–105, 1996.

Foken, T., Göckede, M., Mauder, M., Mahrt, L., Amiro, B. D., and Munger, J. W.: Post-field data quality control, in: Handbook of Micrometeorology: a Guide for Surface Flux Measurement and Analysis, edited by: Lee, X., Massman, W. J., and Law, B., Kluwer, Dordrecht, 181–208, 2004.

Foken, T., Aubinet, M., Finnigan, J., Leclerc, M. Y., Mauder, M., and Paw U, K. T.: Results of a panel discussion about the energy balance closure correction for trace gases, B. Am. Meteorol. Soc., 92, ES13–ES18, doi:10.1175/2011BAMS3130.1, 2011.

Foken, T., Leuning, R., Oncley, S. P., Mauder, M., and Aubinet, M.: Corrections and data quality in: Eddy Covariance: a Practical Guide to Measurement and Data Analysis, edited by: Aubinet, M., Vesala, T., and Papale, D., Springer, Dordrecht, Heidelberg, London, New York, 85–131, 2012a.

Foken, T., Meixner, F. X., Falge, E., Zetzsch, C., Serafimovich, A., Bargsten, A., Behrendt, T., Biermann, T., Breuninger, C., Dix, S., Gerken, T., Hunner, M., Lehmann-Pape, L., Hens, K., Jocher, G., Kesselmeier, J., Lüers, J., Mayer, J.-C., Moravek, A., Plake, D., Riederer, M., Rütz, F., Scheibe, M., Siebicke, L., Sörgel, M., Staudt, K., Trebs, I., Tsokankunku, A., Welling, M., Wolff, V., and Zhu, Z.: Coupling processes and exchange of energy and reactive and non-reactive trace gases at a forest site – results of the EGER experiment, Atmos. Chem. Phys., 12, 1923–1950, doi:10.5194/acp-12-1923-2012, 2012b.

Friend, A. D. and Kiang, N.: Land surface model development for the GISS GCM: effects n improved canopy physiology on simulated climate, J. Climate, 18, 2883–2902, 2005.

Friend, A. D., Stevens, A. K., Knox, R. G., and Cannell, M. G. R.: A process-based, terrestrial biosphere model of ecosystem dynamics (Hybrid v3.0), Ecol. Model., 95, 249–287, 1997.

Gee, G. W., Newman, B. D., Green, S. R., Meissner, R., Rupp, H., Zhang, Z. F., Keller, J. M., Waugh, W. J., van der Velde, M., and Salazar, J.: Passive wick fluxmeters: design considerations and field applications, Water Resour. Res., 45, W04420, doi:10.1029/2008WR007088, 2009.

Gerken, T., Babel, W., Hoffmann, A., Biermann, T., Herzog, M., Friend, A. D., Li, M., Ma, Y., Foken, T., and Graf, H.-F.: Turbulent flux modelling with a simple 2-layer soil model and extrapolated surface temperature applied at Nam Co Lake basin on the Tibetan Plateau, Hydrol. Earth Syst. Sci., 16, 1095–1110, doi:10.5194/hess-16-1095-2012, 2012.

Gerken, T., Babel, W., Sun, F., Herzog, M., Ma, Y., Foken, T., and Graf, H.-F.: Uncertainty in atmospheric profiles and its impact on modeled convection development at Nam Co Lake,

Tibetan Plateau, J. Geophys. Res.-Atmos., 118, 12317–12331, doi:10.1002/2013JD020647, 2013.

Gerken, T., Biermann, T., Babel, W., Herzog, M., Ma, Y., Foken, T., and Graf, H.-F.: A modelling investigation into lake-breeze development and convection triggering in the Nam Co Lake basin, Tibetan Plateau, Theor. Appl. Climatol., in press, doi:10.1007/s00704-013-0987-9, 2014.

Göckede, M., Rebmann, C., and Foken, T.: A combination of quality assessment tools for eddy covariance measurements with footprint modelling for the characterisation of complex sites, Agr. Forest Meteorol., 127, 175–188, 2004.

Göckede, M., Markkanen, T., Hasager, C. B., and Foken, T.: Update of a footprint-based approach for the characterisation of complex measuring sites, Bound.-Lay. Meteorol., 118, 635–655, 2006.

Hafner, S., Unteregelsbacher, S., Seeber, E., Lena, B., Xu, X., Li, X., Guggenberger, G., Miehe, G., and Kuzyakov, Y.: Effect of grazing on carbon stocks and assimilate partitioning in a Tibetan montane pasture revealed by $^{13}CO_2$ pulse labeling, Glob. Change Biol., 18, 528–538, doi:10.1111/j.1365-2486.2011.02557.x, 2012.

Harris, R. B.: Rangeland degradation on the Qinghai-Tibetan plateau: a review of the evidence of its magnitude and causes, J. Arid Environ., 74, 1–12, 2010.

Herzog, M., Oberhuber, J. M., and Graf, H. F.: A prognostic turbulence scheme for the nonhydrostatic plume model ATHAM, J. Atmos. Sci., 60, 2783–2796, 2003.

Hillel, D.: Applications of Soil Physics, Academic Press, New York, 385 pp., 1980.

Holzner, W. and Kriechbaum, M.: Pastures in South and Central Tibet (China), I. Methods for a rapid assessment ofpasture conditions, Bodenkultur, 51, 259–266, 2000.

Hong, J., Kim, J., Ishikawa, H., and Ma, Y.: Surface layer similarity in the nocturnal boundary layer: the application of Hilbert–Huang transform, Biogeosciences, 7, 1271–1278, doi:10.5194/bg-7-1271-2010, 2010.

Hu, J., Hopping, K. A., Bump, J. K., Kang, S., and Klein, J. A.: Climate change and water use partitioning by different plant functional groups in a grassland on the Tibetan Plateau, PLOS ONE, 8, e75503, doi:10.1371/journal.pone.0075503, 2013.

Ingrisch, J., Biermann, T., Seeber, E., Leipold, T., Li, M., Ma, Y., Xu, X., Miehe, G., Guggenberger, G., Foken, T., and Kuzyakov, Y.: Carbon pools and fluxes in a Tibetan alpine *Kobresia pygmaea* grassland partitioned by coupled $^{13}CO_2$ labelling and eddy-covariance measurements, Global Biogeochem. Cy., submitted, 2014.

Ingwersen, J., Steffens, K., Högy, P., Warrach-Sagi, K., Zhunusbayeva, D., Poltoradnev, M., Gäbler, R., Wizemann, H.-D., Fangmeier, A., Wulfmeyer, V., and Streck, T.: Comparison of Noah simulations with eddy covariance and soil water measurements at a winter wheat stand, Agr. Forest Meteorol., 151, 345–355, 2011.

IUSS-ISRIC-FAO: World Reference Base for Soil Resources: a Framework for International Classification, Correlation and Communication, 2nd edn., World soil resources reports, 103, Food and Agriculture Organization of the United Nations, Rome, 128 pp., 2006.

Kaiser, K., Miehe, G., Barthelmes, A., Ehrmann, O., Scharf, A., Schult, M., Schlütz, F., Adamczyk, S., and Frenzel, B.: Turf-bearing topsoils on the central Tibetan Plateau, China: pedology, botany, geochronology, Catena, 73, 300–311, doi:10.1016/j.catena.2007.12.001, 2008.

Kracher, D., Mengelkamp, H.-T., and Foken, T.: The residual of the energy balance closure and its influence on the results of three SVAT models, Meteorol. Z., 18, 647–661, 2009.

Kuzyakov, Y. and Domanski, G.: Carbon input by plants into the soil, review, J. Plant Nutr. Soil Sc., 163, 421–431, 2000.

Liu, W., Wang, X., Zhou, L., and Zhou, H.: Studies on destruction, prevention and control of Plateau Pikas in *Kobresia pygmaea* meadow, Acta Theriol. Sin., 23, 214–219, 2003 (in Chinese with English abstract).

Lloyd, J. and Taylor, J. A.: On the temperature dependence of soil respiration, Funct. Ecol., 8, 315–323, 1994.

Louis, J. F.: A parametric model of vertical fluxes in the atmosphere, Bound.-Lay. Meteorol., 17, 187–202, 1979.

Lundegardh, H.: Ecological studies in the assimilation of certain forest plants and shore plants, Svensk Botaniska Tidskrift, 15, 46–94, 1921.

Ma, Y., Tsukamoto, O., Wang, J., Ishikawa, H., and Tamagawa, I.: Analysis of aerodynamic and thermodynamic parameters on the grassy marshland surface of Tibetan Plateau, Prog. Nat. Sci., 12, 36–40, 2002.

Ma, Y., Kang, S., Zhu, L., Xu, B., Tian, L., and Yao, T.: Roof of the world: Tibetan observation and research platform, B. Am. Meteorol. Soc., 89, 1487–1492, doi:10.1175/2008bams2545.1, 2008.

Mauder, M. and Foken, T.: Documentation and Instruction Manual of the Eddy Covariance Software Package TK2, Arbeitsergebn., Univ. Bayreuth, Abt. Mikrometeorol., 26, 42 pp., 2004.

Mauder, M. and Foken, T.: Documentation and Instruction Manual of the Eddy Covariance Software Package TK3, Arbeitsergebn., Univ. Bayreuth, Abt. Mikrometeorol., 46, 58 pp., 2011.

Mauder, M., Foken, T., Clement, R., Elbers, J. A., Eugster, W., Grünwald, T., Heusinkveld, B., and Kolle, O.: Quality control of CarboEurope flux data – Part 2: Inter-comparison of eddy-covariance software, Biogeosciences, 5, 451–462, doi:10.5194/bg-5-451-2008, 2008.

Mengelkamp, H.-T., Warrach, K., and Raschke, E.: SEWAB a parameterization of the surface energy and water balance for atmospheric and hydrologic models, Adv. Water Res., 23, 165–175, 1999.

Mengelkamp, H. T., Kiely, G., and Warrach, K.: Evaluation of the hydrological components added to an atmospheric land-surface scheme, Theor. Appl. Climatol., 69, 199–212, 2001.

Miehe, G., Kaiser, K., Co, S., and Liu, J.: Geo-ecological transect studies in northeast Tibet (Qinghai, China) reveal human-made mid- Holocene environmental changes in the upper Yellow River catchment changing forest to grassland, Erdkunde, 62, 187–199, doi:10.3112/erdkunde.2008.03.01, 2008a.

Miehe, G., Miehe, S., Kaiser, K., Liu, J. Q., and Zhao, X. Q.: Status and dynamics of *Kobresia pygmaea* ecosystem on the Tibetan plateau, Ambio, 37, 272–279, 2008b.

Miehe, G., Miehe, S., Bach, K., Nölling, J., Hanspach, J., Reudenbach, C., Kaiser, K., Wesche, K., Mosbrugger, V., Yang, Y. P., and Ma, Y. M.: Plant communities of central Tibetan pastures in the Alpine Steppe/*Kobresia pygmaea* ecotone, J. Arid Environ., 75, 711–723, doi:10.1016/j.jaridenv.2011.03.001, 2011.

Miehe, G., Miehe, S., Böhner, J., Kaiser, K., Hensen, I., Madsen, D., Liu, J., and Opgenoorth, L.: How old is the human footprint in the world's largest alpine ecosystem? A review of multiproxy records from the Tibetan Plateau from the ecologists' viewpoint, Quaternary Sci. Rev., 86, 190–209, doi:10.1016/j.quascirev.2013.12.004, 2014.

Mihailovic, D. T., Pielke, R. A., Rajkovic, B., Lee, T. J., and Jeftic, M.: A resistance representation of schemes for evaporation from bare and partly plant-covered surfaces for use in atmospheric models, J. Appl. Meteorol., 32, 1038–1054, 1993.

Mölders, N.: Land-Use and Land-Cover Changes, Impact on Climate and Air Quality, Springer, Dordrecht, Heidelberg, London, New York, 189 pp., 2012.

Moldrup, P., Rolston, D. E., and Hansen, A. A.: Rapid and numerically stable simulation of one dimensional, transient water flow in unsaturated, layered soils, Soil Sci., 148, 219–226, 1989.

Moldrup, P., Rolston, D. E., Hansen, A. A., and Yamaguchi, T.: A simple, mechanistic model for soil resistance to plant water uptake, Soil Sci., 151, 87–93, 1991.

Mügler, I., Gleixner, G., Günther, F., Mäusbacher, R., Daut, G., Schütt, B., Berking, J., Schwalb, A., Schwark, L., Xu, B., Yao, T., Zhu, L., and Yi, C.: A multi-proxy approach to reconstruct hydrological changes and Holocene climate development of Nam Co, Central Tibet, J. Paleolimnol., 43, 625–648, doi:10.1007/s10933-009-9357-0, 2010.

Niu, Y.: The study of environment in the Plateau of Qin-Tibet, Progr. Geogra., 18, 163–171, 1999 (in Chinese with English abstract).

Noilhan, J. and Planton, S.: A Simple parameterization of land surface processes for meteorological models, Mon. Weather Rev., 117, 536–549, 1989.

Oberhuber, J. M., Herzog, M., Graf, H. F., and Schwanke, K.: Volcanic plume simulation on large scales, J. Volcanol. Geoth. Res., 87, 29–53, doi:10.1016/S0377-0273(98)00099-7, 1998.

Reichstein, M.: Drought Effects on Ecosystem Carbon Anwater Exchange in Three Mediterranean Forest Ecosytems – a Combined Top-Down and Bottom-Up Analysis, Bayreuther Forum Ökologie, 89, 1–150, 2001.

Reth, S., Göckede, M., and Falge, E.: CO_2 efflux from agricultural soils in Eastern Germany – comparison of a closed chamber system with eddy covariance measurements, Theor. Appl. Climatol., 80, 105–120, 2005a.

Reth, S., Hentschel, K., Drösler, M., and Falge, E.: DenNit – experimental analysis and modelling of soil N_2O efflux in response on changes of soil water content, soil temperature, soil pH, nutrient availability and the time after rain event, Plant Soil, 272, 349–363, 2005b.

Reth, S., Reichstein, M., and Falge, E.: The effect of soil water content, soil temperature, soil pH-value and the root mass on soil CO_2 efflux – a modified model, Plant Soil, 268, 21–33, 2005c.

Richards, L. A.: Capillary conductivity of liquids in porous mediums, Physics, 1, 318–333, 1931.

Riederer, M.: Carbon fluxes of an extensive meadow and attempts for flux partitioning, Ph.D. thesis, University of Bayreuth, 167 pp., 2014.

Riederer, M., Serafimovich, A., and Foken, T.: Net ecosystem CO_2 exchange measurements by the closed chamber method and the eddy covariance technique and their dependence on atmospheric conditions, Atmos. Meas. Tech., 7, 1057–1064, doi:10.5194/amt-7-1057-2014, 2014.

Shen, M., Zhang, G., Cong, N., Wang, S., Kong, W., and Piao, S.: Increasing altitudinal gradient of spring vegetation phenology during the last decade on the Qinghai–Tibetan Plateau, Agr. Forest Meteorol., 189–190, 71–80, doi:10.1016/j.agrformet.2014.01.003, 2014.

Singh, J. and Gupta, S.: Plant decomposition and soil respiration in terrestrial ecosystems, Bot. Rev., 43, 449–528, 1977.

Staudt, K., Serafimovich, A., Siebicke, L., Pyles, R. D., and Falge, E.: Vertical structure of evapotranspiration at a forest site (a case study), Agr. Forest Meteorol., 151, 709–729, 2011.

Swinnen, J., Vanveen, J. A., and Merckx, R.: C-14 Pulse labeling of field-grown spring whean – an evaluation of its use in rhizosphere carbon budget estimations, Soil Biol. Biochem., 26, 161–170, 1994.

Tanaka, K., Ishikawa, H., Hayashi, T., Tamagawa, I., and Ma, Y.: Surface energy budget at Amdo on the Tibetan Plateau using GAME/Tibet IOP98 data, J. Meteorol. Soc. Jpn., 79, 505–517, 2001.

Tenhunen, J. D., Siegwolf, R. A., and Oberbauer, S. F.: Effects of phenology, physiology, and gradients in community composition, structure, and microclimate on tundra ecosystem CO_2 exchange., in: Ecophysiology of Photosynthesis, edited by: Schulze, E.-D. and Caldwell, M. M., Springer, Berlin, Heidelberg, New York, 431–460, 1995.

Unteregelsbacher, S., Hafner, S., Guggenberger, G., Miehe, G., Xu, X., Liu, J., and Kuzyakov, Y.: Response of long-, medium- and short-term processes of the carbon budget to overgrazing-induced crusts in the Tibetan Plateau, Biogeochemistry, 111, 187–201, doi:10.1007/s10533-011-9632-9, 2012.

van den Bergh, T., Inauen, N., Hiltbrunner, E., and Körner, C.: Climate and plant cover co-determine the elevational reduction in evapotranspiration in the Swiss Alps, J. Hydrol., 500, 75–83, doi:10.1016/j.jhydrol.2013.07.013, 2013.

van Genuchten, M. T.: A closed-form equation for predicting the hydraulic conductivity of unsaturated soils, Soil Sci. Soc. Am. J., 44, 892–898, 1980.

Wei, D., Ri, X., Wang, Y., Wang, Y., Liu, Y., and Yao, T.: Responses of CO_2, CH_4 and N_2O fluxes to livestock exclosure in an alpine steppe on the Tibetan Plateau, China, Plant Soil, 359, 45–55, doi:10.1007/s11104-011-1105-3, 2012.

Wieser, G., Hammerle, A., and Wohlfahrt, G.: The water balance of grassland ecosystems in the Austrian Alps, Arct. Antarct. Alp. Res., 40, 439–445, doi:10.1657/1523-0430(07-039)[WIESER]2.0.CO;2, 2008.

Yang, K., Koike, T., and Yang, D.: Surface flux parameterization in the Tibetan Plateau, Bound.-Lay. Meteorol., 116, 245–262, 2003.

Yang, K., Koike, T., Fuji, H., Tamura, T., Xu, X., Bian, L., and Zhou, M.: The daytime evolution of the atmospheric boundary layer and convection over the Tibetan Plateau: observations and simulations, J. Meteorol. Soc. Jpn., 82, 1777–1792, 2004.

Yang, K., Koike, T., Ye, B., and Bastidas, L.: Inverse analysis of the role of soil vertical heterogeneity in controlling surface soil state and energy partition, J. Geophys. Res., 110, D08101, doi:10.1029/2004JD005500, 2005.

Yang, K., Koike, T., Ishikawa, H., Kim, J., Li, X., Liu, H., Liu, S., Ma, Y., and Wang, J.: Turbulent flux transfer over bare-soil surfaces: characteristics and parameterization, J. Appl. Meteorol. Clim., 47, 276–290, 2008.

Yang, K., Chen, Y.-Y., and Qin, J.: Some practical notes on the land surface modeling in the Tibetan Plateau, Hydrol. Earth Syst. Sci., 13, 687–701, doi:10.5194/hess-13-687-2009, 2009.

Zhang, D., Xu, W., Li, J., Cai, Z., and An, D.: Frost-free season lengthening and its potential cause in the Tibetan Plateau from 1960 to 2010, Theor. Appl. Climatol., 115, 441–450, doi:10.1007/s00704-013-0898-9, 2014.

Zhou, D., Eigenmann, R., Babel, W., Foken, T., and Ma, Y.: Study of near-ground free convection conditions at Nam Co station on the Tibetan Plateau, Theor. Appl. Climatol., 105, 217–228, 2011.

Zhou, H., Zhao, X., Tang, Y., Gu, S., and Zhou, L.: Alpine grassland degradation and its control in the source region of the Yangtze and Yellow Rivers, China, Grassland Sci., 51, 191–203, 2005.

Table 1. Characteristics of the three study sites.

	Xinghai	Kema	Nam Co	
coordinates	35°32′ N, 99°51′ E	31°16′ N, 92°06′ E	30°47″N, 90°60″E	
altitude a.s.l.	3440 m	4410 m	4730 m	
soil (IUSS-ISRIC-FAO, 2006)	Haplic Kastanozems	Stagnic (mollic) Cambisol	Stagnic Cambisols and Arenosol	
pasture type	Montane *Kobresia-Stipa* winter pastures	Alpine *Kobresia pygmaea* pastures	Alpine steppe pastures with mosaic *Kobresia* turfs	
source for soil and plant types	Kaiser et al. (2008), Miehe et al. (2008a), Unteregelsbacher et al. (2012), and Hafner et al. (2012)	This study, Kaiser et al. (2008), Miehe et al. (2011), and Biermann et al. (2011, 2013)	Kaiser et al. (2008), and Miehe et al. (2014)	
climate period	1971–2000	1971–2000	1971–2000	1971–2000
climate station	Xinghai 3323 m a.s.l., 35°35′ N, 99°59′ E	Naqu 4507 m a.s.l., 31°29′ N, 92°04′ E	Baingoin 4700 m a.s.l., 31°23′ N, 90°01′ E	Damxung 4200 m a.s.l., 30°29′ N, 91°06′ E
annual precipitation*	353 mm	430 mm	322 mm	460 mm
mean annual temperature	1.4 °C	−1.2 °C	−0.8 °C	1.7 °C
mean Jul temperature	12.3 °C	9.0 °C	8.7 °C	10.9 °C
source for climate data	http://cdc.cma.gov.cn/			

* Due to the East Asian monsoon, almost all of the precipitation falls in the summer months from May to Sep, most frequently in the form of torrential rain during afternoon thunderstorms.

Table 2. Criteria for a differentiation of main degradation classes at Kema site and survey results.

stage	Intact root Mat (IM)	Degraded root Mat (DM)	Bare Soil (BS)
dominant plant species	*Kobresia pygmaea*	*Kobresia pygmaea*, Lichens, Algae	Annuals, e.g. *Axyris prostrata*
root mat layer	Yes	Yes	No
proportion of total surface area (%, n = 2618)*	65	16	19
mean vegetation cover within the respective stage (%)*	88 ± 6 (SD)	26 ± 10 (SD)	12 ± 8 (SD)
maximal vegetation cover (%)*	99	65	35
minimal vegetation cover (%)*	72	5	0
level difference to BS (cm, n = 60)	9.4 ± 2.0 (SD)	8.5 ± 2.0 (SD)	–

* n = 100 for IM, DM, BS; considered are only "higher graduated plants" (grasses, herbs).

Table 3. Experimental setup during the different experiments, with the corresponding measuring technique and the degree of degradation, (Intact root Mat: IM, Degraded root Mat: DM, Bare Soil: BS, Alpine Steppe: AS).

experiment	eddy-covariance H_2O-, CO_2-flux	micro-lysimeter H_2O-flux	chamber CO_2-flux LI-8100, (R_{eco}, NEE)	^{13}C pulse labeling, ^{13}C chasing
plot area	10^2–10^5 m^2 (footprint)	0.018 m^2	0.031 m^2	0.6 m^2
Xinghai 2009				IM, DM
Nam Co 2009	AS			
Kema 2010	65 % IM, 16 % DM, 19 % BS	IM, BS		IM, DM
Kema 2012		IM, BS	IM, DM, BS	

Table 4. Overview of model scenarios conducted with SEWAB and SVAT-CN for Kema site, periods 2010 and 2012 and Nam Co 2009. The numbers for vegetation fraction and the tile approach have been derived by the classification survey described in Sect. 2.2.

simulation	proportion of total surface area	vegetation cover	model parameter
S_{AS}	100 % Alpine Steppe	0.6	Nam Co AS
S_{IM}	100 % IM	0.88	Kema RM
S_{DM}	100 % DM	0.26	Kema RM
S_{BS}	100 % BS	0.12	Kema BS
S_{RefEC}	tile approach: $S_{RefEC} = 0.65 \cdot S_{IM} + 0.16 \cdot S_{DM} + 0.19 \cdot S_{BS}$		

Table A1. Instrumentation of Kema site in 2010 and 2012 (AWS: Automatic Weather Station).

	complex 1 *Kobresia* pasture, 2010	complex 2* *Kobresia* pasture, 2010	complex 3 bare soil 2010	AWS 2012	radiation and soil complex 2012
wind velocity and wind direction	2.21 m, CSAT3 (Campbell Sci. Ltd.)	2.20 m, CSAT3 (Campbell Sci. Ltd.)	–	2.0 m, WindSonic 1 (Gill)	–
CO_2 and H_2O concentration	2.16 m, LI-7500 (LI-COR Biosciences)	2.19 m, LI-7500 (LI-COR Biosciences)	–	–	–
air temperature and humidity	2.20 m, HMP 45 (Vaisala)	2.20 m, HMP 45 (Vaisala)	–	2.0 m, CS 215 (Campbell Scientific Ltd.)	–
ambient pressure	–	inside Logger Box (Vaisala)	–	–	–
solar radiation	1.90 m, CNR1 (Kipp & Zonen)	1.88 m; CNR1 (Kipp & Zonen)	–	2.0 m, Pyranometer SP 110 (Apogee), NR Lite (Kipp & Zonen), LI 190 SB (LI-COR)	2.0 m; CNR1 (Kipp & Zonen)
precipitation	–	1.0 m, Tipping bucket	–	0.5 m, Tipping Bucket (Young)	–
soil moisture	−0.15, Imko-TDR	−0.1, −0.2, Imko-TDR	−0.15, Imko-TDR	−0.05, −0.125, −0.25, Campbell CS 616	−0.1, −0.2, Imko-TDR
soil water potential	–	–	–	−0.05, −0.125 −0.25 Campbell 257-L	–
soil temperature	−0.025, −0.075, −0.125, Pt 100	−0.025, −0.075, −0.125, −0.2, Pt 100	−0.025, −0.075, −0.125, Pt 100	−0.025, −0.075 −0.125, −0.25, Pt 100	−0.025, −0.075, −0.125, −0.175, Pt 100
soil heat flux	−0.15, HP3	−0.15, HP3	−0.15, HP3	–	−0.2, HP3, Hukseflux

* This complex was used due to the higher data availability. There was no difference between the two instruments.

Table A2. Instrumentation of NamCo site in 2009 (only relevant instruments are shown).

device	type/manufacturer	height
ultrasonic anemometer	CSAT3 (Campbell Scientific Ltd.)	3.1 m
gas analyser	LI-7500 (LI-COR Biosciences)	3.1 m
temperature-humidity sensor	HMP 45 (Vaisala)	3.1 m
net-radiometer	CM3 & CG3 (Kipp&Zonen)	1.5 m
rain gauge	tipping bucket	1 m
soil moisture	Imko-TDR	−0.1, −0.2, −0.4, −0.8, −1.60
soil Temperature	Pt100	−0.2, −0.4, −0.8, −1.60
logger	CR5000 (Campbell Scientific Ltd.)	

Table C1. Relevant parameters to describe the surface characteristic in SEWAB and SVAT-CN. Kema represents two parameter sets, (i) root mat (RM) for IM and DM, and (ii) BS.

parameter	unit	description	SEWAB			SVAT-CN		
			Kema RM	Kema BS	NamC AS	Kema RM	Kema BS	NamC AS
a	–	albedo	0.18[a] 0.16[b]	0.18[a] 0.148[b]	0.196	0.18[a] 0.16[b]	0.18[a] 0.148[b]	0.196
ε	–	emissivity	0.97	0.97	0.97	0.97	0.97	0.97
f_{veg}	–	fraction of vegetated area	0.88 (IM) 0.26 (DM)	0.12	0.6	0.88 (IM) 0.26 (DM)	0.12	0.6
LAI	–	leaf area index	1.0	1.0	1.0	0.5[a] 1.0[b]	0.5[a] 1.0[b]	1.0
z_r	m	root depth	0.5	0.3	0.3	0.4	0.4	0.4
h_c	m	canopy height	0.03	0.03	0.15	0.03	0.03	0.15
z_{om}	m	roughness length	0.003	0.003	0.005	0.003	0.003	0.005
$R_{s,\,min}$	$s\,m^{-1}$		72	72	60	[c]	[c]	[c]
$R_{s,\,max}$	$s\,m^{-1}$		2500	2500	2500	[c]	[c]	[c]
$\lambda_{s,\,dry}$	$W\,m^{-1}\,K^{-1}$	thermal conductivity, dry soil	0.15	0.15	0.15	[c]	[c]	[c]
	$W\,m^{-1}\,K^{-1}$	thermal conductivity at saturation	0.8	1.3	1.3	[c]	[c]	[c]
$C_G \cdot \rho_G$	$10^6\,J\,m^{-3}\,K^{-1}$	soil heat capacity (solid matter)	2.34	2.1	2.1	2.4	2.4	2.4
Θ_{sat}	$m^3\,m^{-3}$	porosity	0.593	0.533	0.396	0.593[d] 0.533[e]	0.533	0.396
Ψ_{sat}	m	matrix potential at saturation	−0.074	−0.022	−0.51	[c]	[c]	[c]
K_{sat}	$10^{-5}\,m\,s^{-1}$	saturated hydraulic conductivity	1.90	4.60	2.02	1.90	4.60	2.02
Θ_{FC}	$m^3\,m^{-3}$	volumetric water content at field capacity	0.252	0.201	0.210	[c]	[c]	[c]
Θ_{WP}	$m^3\,m^{-3}$	volumetric water content at wilting point	0.088	0.087	0.060	[c]	[c]	[c]
b	–	exponent[f]	4.38	5.54	3.61	[c]	[c]	[c]
θ_r	$m^3\,m^{-3}$	soil residual water content[g]	[c]	[c]	[c]	0.025[d] 0.05[e]	0.05	0.025
α	m^{-1}	scale parameter[g]	[c]	[c]	[c]	0.006[d] 0.003[e]	0.003	0.0466
n	–	shape parameter[g]	[c]	[c]	[c]	1.17[d] 1.27[e]	1.27	1.443

[a] from measurements in 2010,
[b] from measurements in 2012,
[c] parameter not available due to different parameterization,
[d] organic layer (0–15 cm depth),
[e] mineral layer (15+ cm depth),
[f] exponent b for relationships after Clapp and Hornberger (1978),
[g] parameter according to van Genuchten (1980).

Table C2. Parameters applied to describe leaf physiology of *Kobresia pygmaea*. For detailed explanation of the leaf model and use of the parameters see Falge (1997). Output of the model is on a projected leaf area basis.

description	parameter	value original	value Kema	value NamCo	unit
dark respiration	$F(R_d)$	1.51	2.42	1.51	$\mu mol\ m^{-2}\ s^{-1}$
	$E_a(R_d)$	72 561			$J\ mol^{-1}$
electron transport capacity	$c(P_{ml})$	61.93	99.1	28.0	$\mu mol\ m^{-2}\ s^{-1}$
	$\Delta H_a(P_{ml})$	50 224			$J\ mol^{-1}$
	$\Delta H_d(P_{ml})$	200 000			$J\ mol^{-1}$
	$\Delta S(P_{ml})$	436.8			$J\ K^{-1}\ mol^{-1}$
carboxylase capacity	$c(Vc_{max})$	53.4	85.4	32.5	$\mu mol\ m^{-2}\ s^{-1}$
	$\Delta H_a(Vc_{max})$	41 953			$J\ mol^{-1}$
	$\Delta H_d(Vc_{max})$	200 000			$J\ mol^{-1}$
	$\Delta S(Vc_{max})$	206.1			$J\ K^{-1}\ mol^{-1}$
carboxylase kinetics	$f(K_c)$	299.469			$\mu mol\ mol^{-1}$
	$E_a(K_c)$	65 000			$J\ mol^{-1}$
	$f(K_o)$	159.597			$mmol\ mol^{-1}$
	$E_a(K_o)$	36 000			$J\ mol^{-1}$
	$f(\tau)$	2339.53			–
	$E_a(\tau)$	−28 990			$J\ mol^{-1}$
light use efficiency	α	0.0332	0.0332	0.0111	$(mol\ CO_2)\ (mol\ photons)^{-1}$
stomatal conductance	g_{min}	18.7			$mmol\ m^{-2}\ s^{-1}$
	$gfac_0$	21			–

For Kema site, the respective formulation was adapted to: $gfac = \max(15, gfac_0 \times 10^{(0.025 \cdot \Psi)})$, Ψ in MPa, simulated in 10 cm depth.

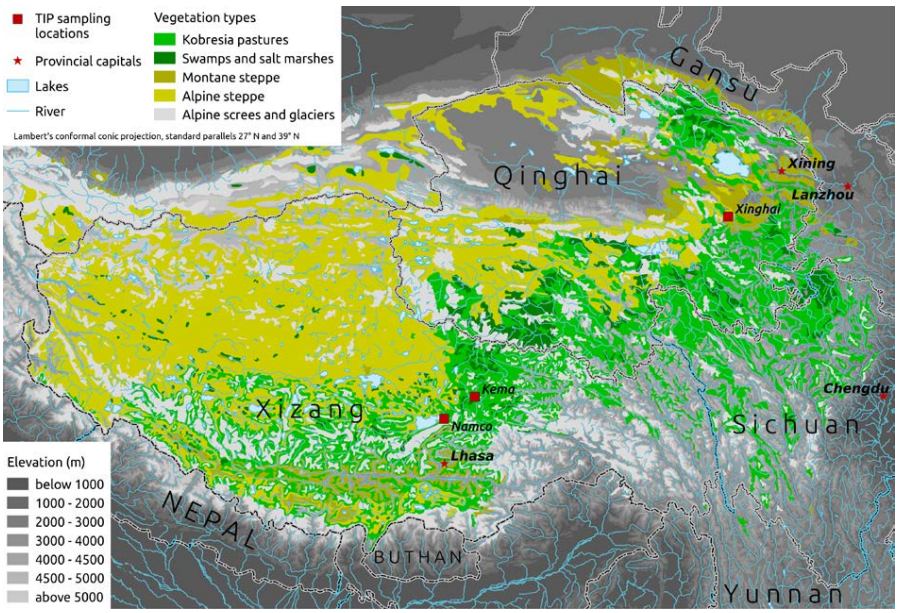

Figure 1. *Kobresia pygmaea* pastures (in green) dominate the southeastern quarter of the Tibetan highlands, whereas the alpine steppe covers the arid northwestern highlands. The experimental sites Xinghai and Kema are in montane and alpine *Kobresia* pastures, whereas the Nam Co site is situated in the ecotone towards alpine steppe (modified after Miehe et al., 2008b).

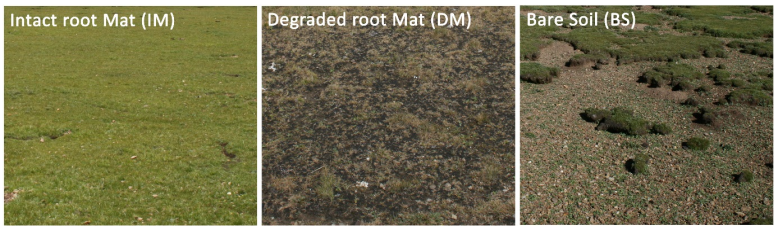

Figure 2. The three defined vegetation classes, **(a)** intact root Mat (IM), **(b)** degraded root Mat (DM) and **(c)** Bare Soil (BS).

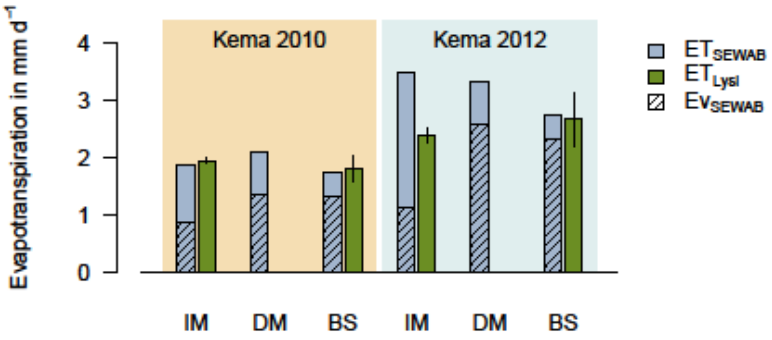

Figure 3. Evapotranspiration (ET) derived with SEWAB and with micro-lysimeter measurements at Kema in 2010 (33 days: 23 June–25 July) and Kema in 2012 (40 days: 16 July–24 August) for intact root mat (IM), degraded root mat (DM) and bare soil (BS). Hatched bars denote the simulated evaporation (Ev) as part of the total simulated ET, the remainder is transpiration. Black lines on top of the bars for the micro-lysimeter illustrate standard deviations ($n = 4$).

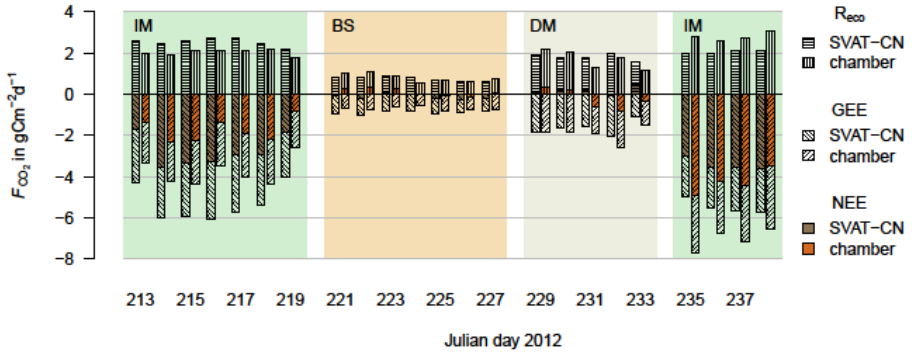

Figure 4. Comparison of measured and modelled daily carbon exchange sums from 31 July to 25 August 2012 at Kema. Hatched bars denote the simulated gross ecosystem exchange (GEE) and ecosystem respiration (R_{eco}), the sum is the net ecosystem exchange (NEE, coloured bars). The four periods represent different stages of vegetation degradation (see Table 2). Leaf physiology and soil respiration was parameterized for best representation of the gas exchange chamber data over the entire time period (see Sect. 2.5.2). Missing dates indicate days, when chambers were set up or relocated to another treatment.

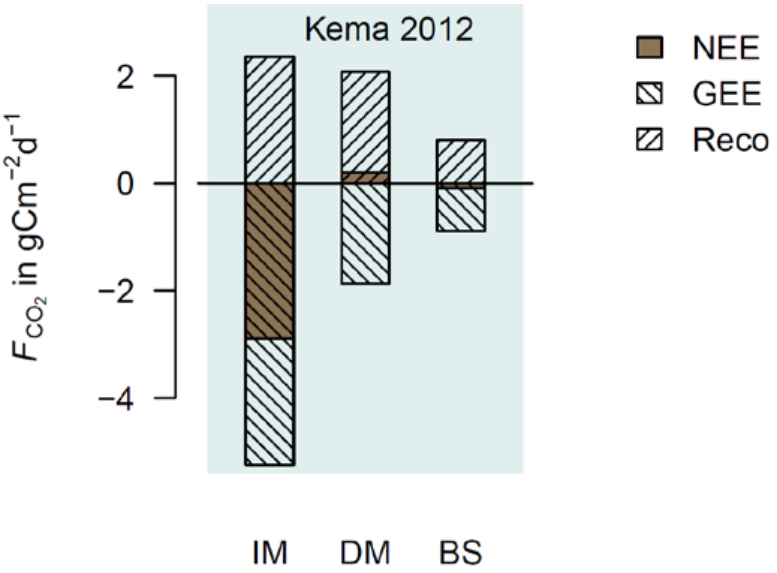

Figure 5. Simulated carbon fluxes at Kema in 2012 (46 days: 12 July to 26 August 2012) for IM, DM, and BS. Hatched bars denote the simulated GEE and R_{eco}, the sum is the NEE (brown bar).

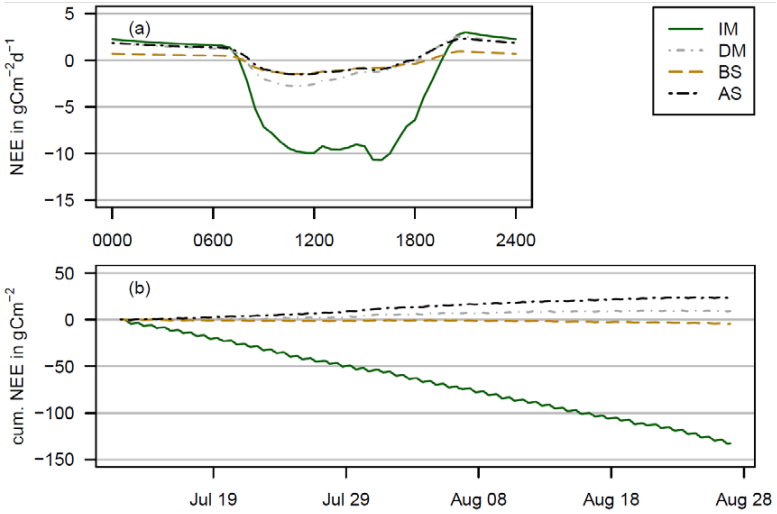

Figure 6. Model results of net ecosystem exchange (NEE) over 46 days of July and August 2012 at Kema. **(a)**: mean diurnal cycle, and **(b)**: cumulative NEE. The four lines represent different stages of vegetation degradation (IM, DM, BS, and AS).

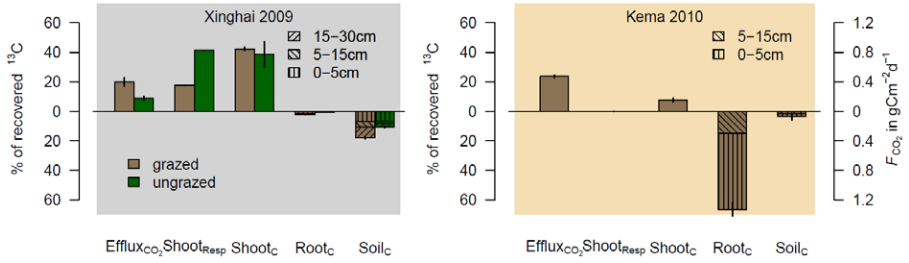

Figure 7. ^{13}C partitioning and distribution of recently allocated C within the various pools, namely CO_2 efflux, shoot respiration, shoots, roots and soil for Xinghai site (grazed and ungrazed) in 2009 and Kema site (IM) in 2010, determined at the end of a 29 day and 15 day allocation period, respectively. Total fluxes of C in g C m^{-2} d^{-1} to the different C pools at Kema site are based on the combination of eddy-covariance measurements and labelling. Shoot respiration is not measured, but determined as difference between the ^{13}C recovery at the first sampling and the sampling at the end of the allocation period. First sampling in Xinghai was one day after the labelling and in Kema at the labelling day. Figure modified after Hafner et al. (2012) and Ingrisch et al. (2014).

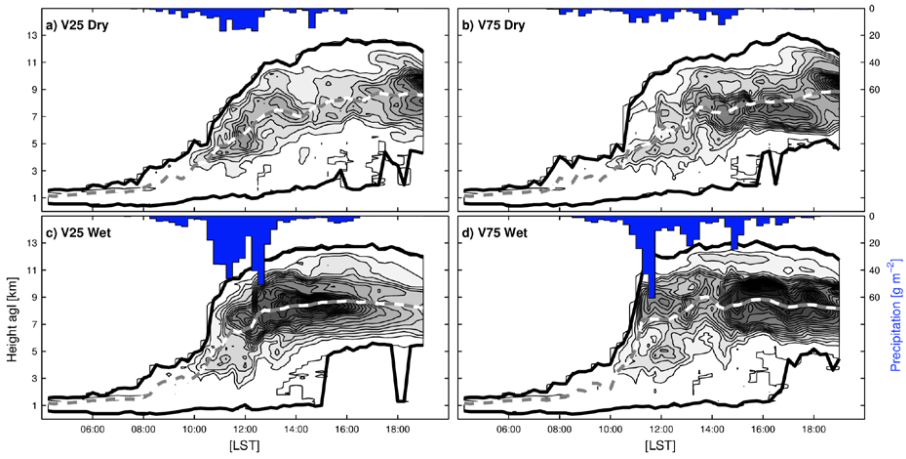

Figure 8. Simulated convection development and deposited precipitation (blue bars) for a symmetric Tibetan Valley with 150 km width. The black lines indicate cloud base and cloud top in kilometres above ground level, the dashed line shows the centre of the cloud mass and the contours give the mean cloud water and ice concentration integrated over the model domain. V25 and V75 refer to 25 % and 75 % vegetation cover, while wet and dry indicate initial soil moistures corresponding to 1.0 and 0.5× field capacity, respectively.

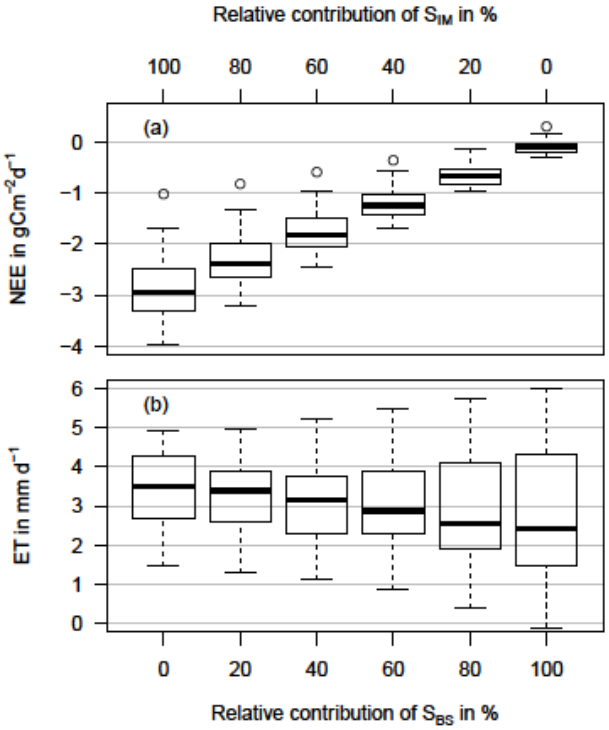

Figure 9. Modelled daily net ecosystem exchange (a, NEE) and modelled daily evapotranspiration (b, ET) for 46 days (12 July to 26 August 2012) at Kema (varying combination of S_{IM} and S_{BS}): box plot with median, 25 % and 75 % quartiles; bars represent quartiles ±1.5 times interquartile range.

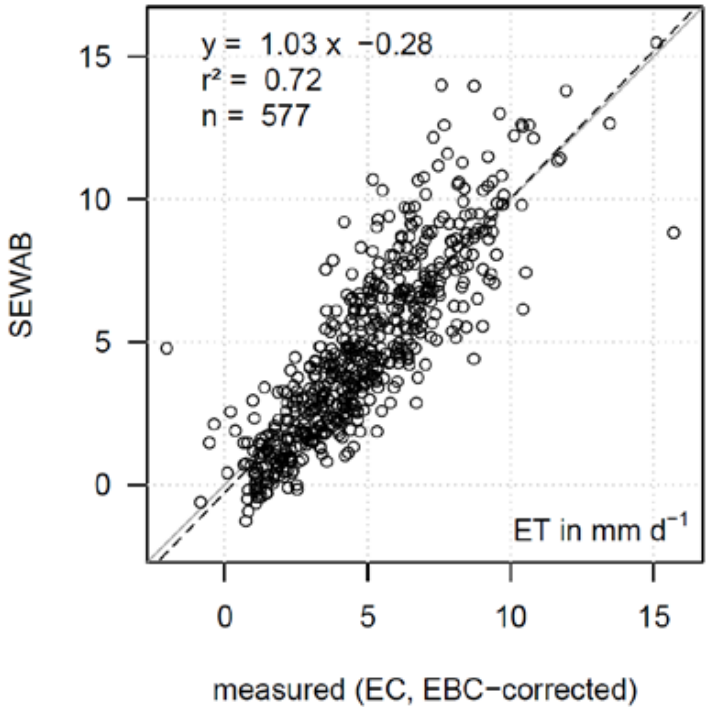

Figure D1. Scatterplot of measured vs. SEWAB modelled S_{RefEC} evapotranspiration (ET) over 61 days of 2010 (3 June to 2 August) at Kema. Measured and modelled values are restricted to high data quality (flag 1–3 out of a scheme ranging from 1–9, Foken et al., 2004). Measured EC data is corrected according to the surface energy imbalance with the buoyancy flux correction.

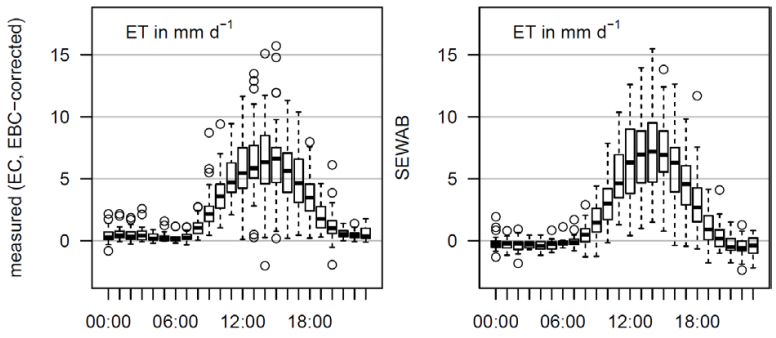

Figure D2. Mean diel course of measured and energy balance corrected evapotranspiration ET (left panel) and SEWAB modelled ET (Tile approach according to the EC footprint: S_{RefEC}, right panel) over 61 days of 2010 (3 June to 2 August) at Kema: box plot with median, 25 % and 75 % quartiles; bars represent quartiles ±1.5 times interquartile range, dots are outliers. Measured and modelled values are restricted to high flux data quality (flag 1–3). Measured data is corrected according to the surface energy imbalance with the buoyancy flux correction.

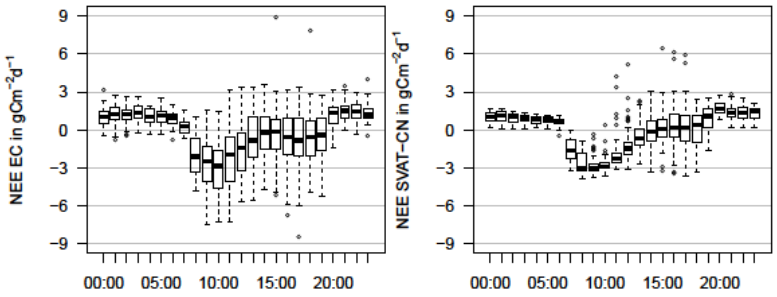

Figure D3. Mean diel course of measured (left panel) and modelled (tile approach according to the EC footprint: S_{RefEC}, right panel) net ecosystem exchange (NEE) over 61 days of 2010 (3 June to 2 August) at Kema: box plot with median, 25 % and 75 % quartiles; bars represent quartiles ±1.5 times interquartile range, dots are outliers. Measured and modelled values are restricted to high data quality (flag 1–3 out of a scheme ranging from 1–9, Foken et al., 2004).

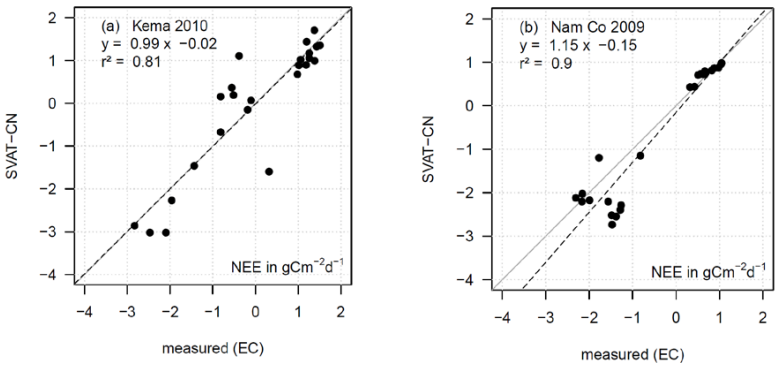

Figure D4. Comparison of hourly medians (see Fig. D3) of measured and modelled net ecosystem exchange for the 2010 campaign at Kema (left panel) and 2009 campaign at Nam Co (right panel). The regression line (dashed, black) is shown as well as the 1 : 1 line (solid, gray).

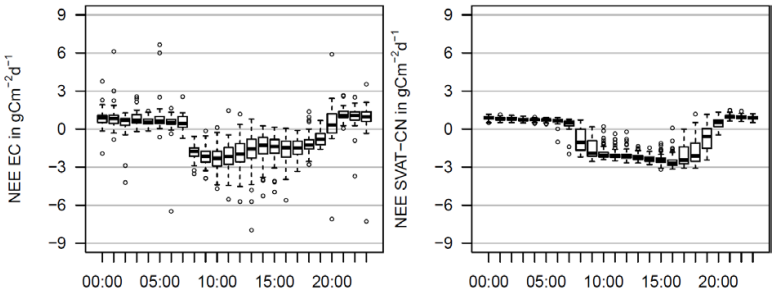

Figure D5. Mean diel course of measured (left panel) and modelled (right panel) net ecosystem exchange (NEE) over 44 days of 2009 (26 June to 8 August) at Nam Co: box plot with median, 25 % and 75 % quartiles; bars represent quartiles ±1.5 times interquartile range, dots are outliers. Measured and modelled values are restricted to high data quality (flag 1–3 out of a scheme ranging from 1–9, Foken et al., 2004). Model parameters for leaf physiology and soil respiration were adapted for best representation of eddy covariance data (see Sect. 3.2.1).